Synthesis and Characterization of Germanium, Tin, Phosphorus, Iron, and Rhodium Complexes of Tris(pentafluorophenyl)corrole, and the Utilization of the Iron and Rhodium Corroles as Cyclopropanation Catalysts

Liliya Simkhovich,[a] Atif Mahammed,[a] Israel Goldberg,*[b] and Zeev Gross*[a]

Abstract: The germanium(IV), tin(IV), and phosphorus(V) complexes of tris(pentafluorophenyl)corrole were prepared and investigated by electrochemistry for elucidation of the electrochemical HOMO–LUMO gap of the corrole and the spectroscopic characteristics of the corrole π radical cation. This information was found to be highly valuable for assigning the oxidation states in the various iron corroles that were prepared. Two iron corroles and the rhodium(I) complex of an *N*-substituted corrole were fully characterized by X-ray crystallography and all the transition metal corroles were examined as cyclopropanation catalysts. All iron (except the NO-ligated) and rhodium corroles are excellent catalysts for cyclopropanation of styrene, with the latter displaying superior selectivities. An investigation of the effect of the oxidation state of the metal and its ligands leads to the conclusion that for iron corroles the catalytically active form is iron(III), while all accesible oxidation states of rhodium are active.

Keywords: catalysts · corroles · cyclopropanations · iron · N ligands · rhodium

Introduction

Corroles are tetrapyrrolic macrocycles that are closely related to porphyrins, with one carbon atom less in the outer periphery and one NH proton more in their inner core.[1] They may also be considered as the aromatic version (identical skeleton) of the only partially conjugated corrin, the cobalt-coordinating ligand in Vitamin B_{12} (Scheme 1). Accordingly, it is not surprising that corroles have been known for more than 35 years and that many aspects of their coordination chemistry have been explored.[2] The somewhat contracted coordination core of corroles and the fact that they act as trianionic ligands leads to what is the most outstanding feature of corroles relative to porphyrins and other organic ligands, that is, the stabilization of metal ions in high oxidation states. The most relevant examples from the first-row transition metals include complexes of electron-rich corroles with chromium(V),[3] iron(IV),[4] cobalt(IV), and even cobalt(V).[5] This phenomenon is especially surprising, since the corrole macrocycle itself is oxidized at much lower potentials than analogous porphyrins. For example, the oxidation potentials of $[Sn(oep)Cl_2]$ (**1**) and [Sn(oec)Cl] (**2a**) are 1.36

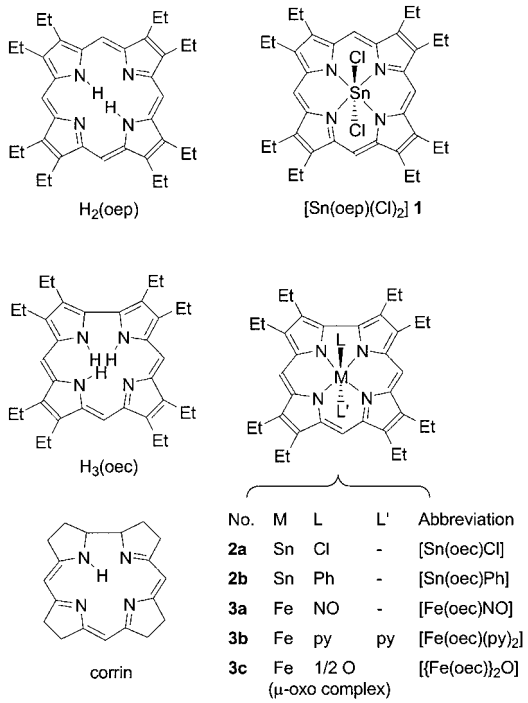

Scheme 1. The formulae of corrin, octaethylporphyrin, octaethylcorrole, and of the metal complexes that are mentioned in the text.

[a] Prof. Dr. Z. Gross, L. Simkhovich, Dr. A. Mahammed
Department of Chemistry and
Institute of Catalysis Science and Technology
Technion—Israel Institute of Technology
Haifa 32000 (Israel)
Fax: (+972) 4-823-3735
E-mail: chr10zg@tx.technion.ac.il

[b] Prof. Dr. I. Goldberg
School of Chemistry, Tel Aviv University
Tel Aviv 69978 (Israel)

  0947-6539/01/0705-1041 $ 17.50+.50/0

and 0.67 V, respectively (for the abbreviations, see Scheme 1).[6] Accordingly, one would expect the oxidation site ambiguity (metal^n/metal^{n+1} vs macrocycle/macrocycle$^{\bullet+}$) to be much more pronounced in transition metal corroles than in corresponding metalloporphyrins. However, radical complexes of transition metal corrole are actually rare, with the two most unambiguous examples being the one-electron oxidation products of (chloro)iron(IV) and (nitrosyl)iron(III) corroles.[7] Another example is the temperature-dependent oxidation-site preference of copper(III) corrole versus copper(II) corrole radical.[8] In addition, it has been suggested that the formally iron(IV) and manganese(III) corroles may actually be more appropriately described as iron(III) and manganese(II) corrole radicals, respectively.[9] Similar paradoxical situations in metalloporphyrins have been resolved through extensive investigations of non transition metal (especially zinc and magnesium) complexes of porphyrin radicals and revelation of their characteristic spectroscopic features.[10]. However, much less is currently known about the analogous corrole radicals, simply because only very few non-transition metal corroles have been reported (In^{III}, Ge^{IV}, Sn^{IV}, P^{V}),[11] and of these only the tin complexes were investigated in this respect.[6, 12]

The metal versus macrocycle oxidation ambiguity is particularly important in catalysis, during which the catalysts are frequently involved in redox processes. Although corrole–metal complexes were not utilized in any catalytic application until most recently,[13] this situation is changing now as increasingly simple methods of corrole synthesis are introduced.[14] We have contributed to this field by disclosing a highly facile synthesis of tris(pentafluorophenyl)corrole[15] (H_3(tpfc); **4** in Scheme 2).[16] Subsequently, we have demonstrated that both its iron and manganese complexes are potent oxidation catalysts, with isolable oxomanganese(V) in the latter case.[13, 17] As for cyclopropanation of olefins by carbenoids, the iron(IV) and rhodium(III) corroles were shown to be much better catalysts than analogous porphyrins.[13] We have also reported the X-ray crystal structures of the two last-mentioned complexes, [Fe^{IV}(tpfc)Cl] (**5b**) and [Rh^{III}(tpfc)-$(PPh)_3$] (**6a**),[18] as well as that of [Cr^{V}(tpfc)O].[19] In addition, we have demonstrated that chiral ligands are easily prepared from **4**, through the alkylation of one of its three inner NHs.[20] In principle, this opens up the possibility of using metal complexes of *N*-substituted corroles as catalysts for asymmetric synthesis. All these developments call for an extensive investigation of the metal complexes of **4** in terms of structural characterizations, electronic structures, and reaction mechanisms of their action in the catalytic processes. Accordingly, we now report the preparation of the iron complexes of **4** in various oxidation and coordination states, including the X-ray structures of the binuclear μ-oxo iron(IV) and the mononuclear bis-pyridine-coordinated iron(III) corroles. In addition, we report the germanium(IV), tin(IV), and phosphorus(V) complexes of **4**, and their one-electron oxidation products. These investigations, together with the electrochemistry of all the complexes, disclose some characteristics of corrole radicals and support the conclusion that the corrole is not oxidized in any of the iron complexs isolated in this study (**5a**–**5e**). In combination with the results of cyclopropanation catalysis by the various iron corroles, it also suggests that the reactive species in the process is invariably the mononuclear

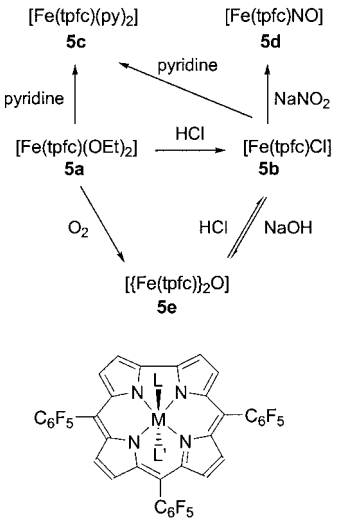

No.	M	L	L'	Abbreviation
4	3H	-	-	H_3(tpfc)
5a	Fe	OEt	OEt	[Fe(tpfc)$(OEt)_2$]
5b	Fe	Cl	-	[Fe(tpfc)Cl]
5c	Fe	py	py	[Fe(tpfc)$(py)_2$]
5d	Fe	NO	-	[Fe(tpfc)NO]
5e	Fe	1/2 O (μ-oxo complex)	-	[{Fe(tpfc)}$_2$O]
6a	Rh	PPh_3	-	[Rh(tpfc)PPh_3]
6b	Rh	$P(C_6H_{11})_3$	-	[Rh(tpfc)$P(C_6H_{11})_3$]
7a	Ge	Cl	-	[Ge(tpfc)Cl]
7b	Ge	OH	-	[Ge(tpfc)OH]
8	Sn	Cl	-	[Sn(tpfc)Cl]
9	P	OH	OH	[P(tpfc)$(OH)_2$]

Scheme 2. Formulae of 5,10,15-tris(pentafluorophenyl)corrole and its metal complexes, and the interconversion of the various iron corroles.

Abstract in Hebrew:

במסגרת עבודה זו הוכנו לראשונה קומפלקסים של טריס(פנטאפלואורופניל)קורול עם גרמניום(IV), בדיל(IV), וזרחן(V) ששימשו לקביעת ההפרשים האנרגטיים בין אורביטלי HOMO ו-LUMO של הקורול (באמצעות אלקטרוכימיה) והמאפיינים הספקטרוסקופיים של קורול קטיון רדיקלים. מידע זה היה לעזר רב בקביעת מצבי החמצון של הברזל קורולים המגוונים שהוכנו. שני ברזל קורולים וקומפלקס הרודיום(I) של קורול *N*-מותמר אופיינו במלואם בקריסטלוגרפיה של קרני X וכל קומפלקסי מתכות המעבר נבחנו כזרזים לציקלופרופנציה. כל קומפלקסי הברזל (מלבד זה הקשור ל-NO) והרודיום הינם זרזים מצוינים עבור ציקלופרופנציה של סטירן, כאשר הקומפלקס האחרון הינו בעל סלקטיביות עדיפה. חקירת ההשפעה של מצבי חמצון המתכת והליגנדות שלה מובילה למסקנה שעבור ברזל קורולים הצורה הפעילה של הזרז היא ברזל תלת-ערכי ועבור רודיום כל מצבי החמצון הזמינים הינם פעילים.

0947-6539/01/0705-1042 $ 17.50+.50/0 *Chem. Eur. J.* **2001**, *7*, No. 5

iron(III) complex. Finally, we present also the highly efficient cyclopropanation catalysis by rhodium corroles together with the X-ray structure of a rhodium complex of an *N*-substituted corrole and the results of the attempted trapping of reaction intermediates.

Results and Discussion

Synthesis and characterization of the iron complexes of 5,10,15-tris(pentafluorophenyl)corrole (H_3(tpfc) (4)) in various oxidation and coordination states: We, as well as Vogel and co-workers, have previously shown that the most stable oxidation state of iron in corroles is +4.[4, 18] We have now found that it is possible to use one common starting point for the synthesis of many iron complexes of **4**, and controlling the oxidation state of iron and its ligands by either the adopted workup procedure or the interconversions shown in Scheme 2.

The first synthetic step consists of heating a solution of **4** in DMF with iron(II) chloride, followed by evaporation of the solvent. As long as some residual DMF, or any other coordinating ligand is present, the complex remains protected from oxidation to iron(IV). The most convenient way for isolation of the complex in the iron(III) oxidation state is to wash the solid residue with diethyl ether, elute the resulting solution through a silica column with diethyl ether, and evaporate the solution to dryness (a brownish solid is obtained). This allows the isolation of [Fe(tpfc)$(OEt_2)_2$] (**5a**), which is air-stable in the solid state and in solutions that contain about 20% diethyl ether. The ^{1}H NMR spectrum of **5a** displays four paramagnetically shifted and broadened resonances for the pyrrole-H resonances (Figure 1a), two of which are located at low field. This is consistent with intermediate-spin iron(III), since all resonances are expected at low field for pure high-spin iron(III), while the reverse holds for low-spin complexes.[21] The EPR spectrum of **5a** with $g =$ 3.8 (Figure 1c, observable at RT in the solid state and in frozen solutions) also supports this conclusion, as may be deduced from the extensive work with iron(III) porphyrins (high-spin: $g_\perp \approx 6$, $g_\parallel \approx 2$, intermediate-spin: $g_\perp \approx 4$, low-spin: $g_z > 2$, $g_y \approx 2$, $g_x < 2$).[22] Finally, the ^{19}F NMR spectrum shown in Figure 1b displays three sets of resonances, all in a 2:1 ratio due to the different magnetic environment of the central C_6F_5 ring relative to the two other. All resonances may be assigned to specific fluorine atoms, based on an expected decrease in both linewidths and paramagnetic shifting from the diamagnetic positions as a function of their distance of from the metal [the chemical shifts of *meta*-, *para*-, and *ortho*-F atoms in diamagnetic complexes of **4** (see Figures 4 and 5 later) are about $\delta = -138, -155, -162$, respectively].

Isolation of [Fe(tpfc)$(py)_2$] (**5c**) follows an identical route, but the final crystallization is performed from diethyl ether and heptane in the presence of pyridine. This complex is much more stable to oxidation, that is, even without a large excess of ligand. The ^{1}H NMR spectrum of **5c** shown in Figure 2a discloses low-field resonances due to the coordinated pyridine ligands (exchangeable by [D_5]pyridine), while only high-field-shifted pyrrole-H resonances are obtained (at $\delta = +3, -61,$

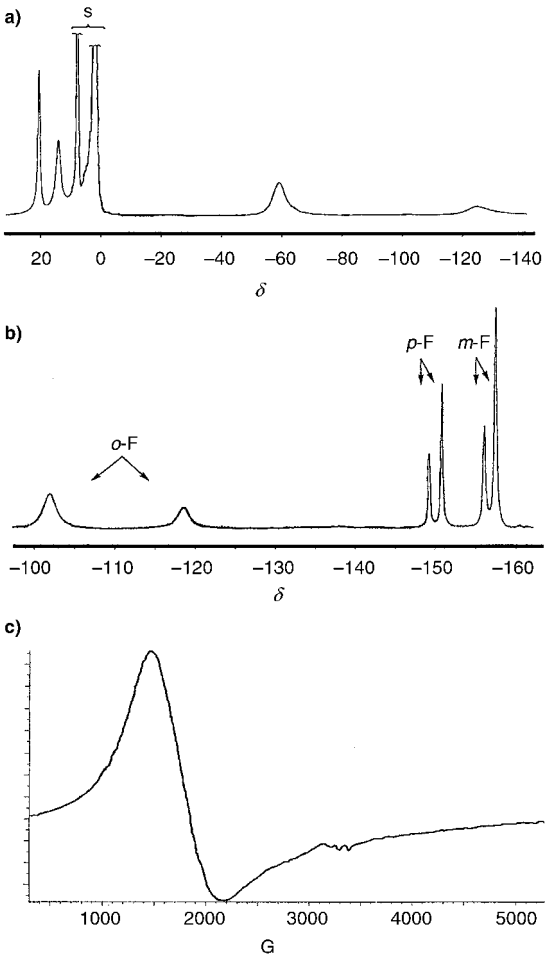

Figure 1. Spectroscopic features of [Fe(tpfc)$(OEt_2)_2$] (**5e**): a) ^{1}H NMR (25 °C, [D_6]benzene, s stands for solvent impurities), b) ^{19}F NMR (25 °C, [D_6]benzene), c) EPR (powder, 130 K).

-66, and -135). The direction of the paramagnetic shifts and the large spread therein are consistent with low-spin iron(III) in a highly rhombic coordination environment.[22] Furthermore, the relatively small linewidths in both the ^{1}H and ^{19}F NMR spectra (compare the spectra in Figure 2 and Figure 1) also support this conclusion, as the relaxation rate (mainly affected by the electron spin-lattice relaxation time T_{1e}) in such complexes is known to be very high.[23] The last phenomenon is also the reason for the absence of an EPR spectrum down to 130 K. Finally, we have examined a crystal of **5c** by X-ray crystallography. Although the resolution is quite low, because of the presence of an additional non-coordinated and disordered pyridine in the lattice (there is also a rotational disorder of the central aryl ring, even at 120 K), it still allows the confirmation of the basic structural features suggested by the spectroscopic analysis. These are the almost perfect mutual linear alignment of the coordinated pyridines (Figure 2c), together with the relative flatness of the macrocycle and some short Fe–N(pyrrole) bond lengths (see Table 1 for comparison with the two other iron complexes of **4**), which are all characteristic of low-spin iron(III) in a highly rhombic coordination environment.[22, 24]

The iron(IV) complexes are obtained by performing the work up procedure with noncoordinating solvents (CH_2Cl_2 or

Table 1. Selected structural parameters for the analyzed iron complexes of **4**.

	[Fe(tpfc)Cl] (**5b**)[18]	[{Fe(tpfc)}$_2$O] (**5e**)[c]	[Fe(tpfc)(py)$_2$] (**5c**)
Fe–N(corrole) bond length range [Å]	1.880 – 1.922(6)	1.884 – 1.923(5) 1.888 – 1.929(5)	1.865 – 1.923(5)
Fe–axial-ligand bond lengths [Å]	2.238(2)	1.709(4) 1.726(4)	2.028, 2.032(5)
Fe deviations from the N$_4$(corrole) plane [Å]	0.367(1)	0.421(1) 0.426(1)	0.001(1)
twist angles [°] between adjacent pyrrole rings[a]	2.1, 6.5, 5.8, 8.7(3)	4.0, 8.4, 3.7, 9.4(2) 4.6, 12.8, 1.7, 9.5(2)	3.4, 1.5, 3.4, 5.4(2)
puckering of the corrole rings[b]	− 0.17 to + 0.13	− 0.14 to + 0.13 − 0.24 to + 0.17	− 0.09 to + 0.10

[a] Within the ring sequence $N^{21} \cdots N^{22} \cdots N^{23} \cdots N^{24} \cdots N^{21}$. [b] Deviation range [Å] of individual atoms from the 21-atom corrole core ring. [c] Data for the two independent corrole rings are listed in separate lines.

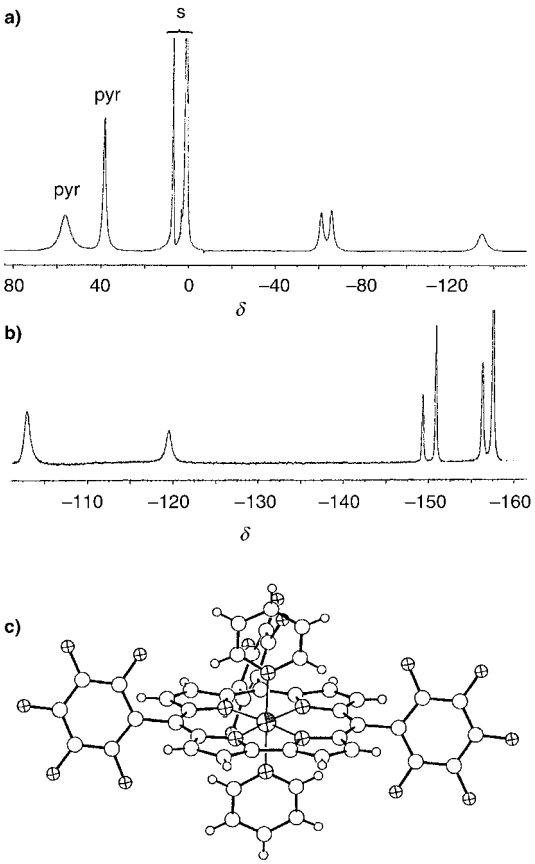

Figure 2. Characterization of [Fe(tpfc)(py)$_2$] (**5c**) by a) ^{1}H NMR (25 °C, [D$_6$]benzene, s stands for solvent impurities and py for coordinated pyridine), b) ^{19}F NMR (25 °C, [D$_6$]benzene), c) X-ray crystallographic structure.

benzene), during which oxidation to a mixture of mononuclear and binuclear products occurs rapidly. Washing such mixtures with either aqueous HCl or NaOH allows the isolation of the paramagnetic [Fe(tpfc)Cl] (**5b**) and the diamagnetic [{Fe(tpfc)}$_2$O] (**5e**), respectively. Both iron(IV) complexes were fully characterized by X-ray crystallography; that of **5b** has already been reported[18] and that of **5e** is shown in Figure 3 together with its ^{19}F NMR spectrum.

The combination of the NMR spectrum and the crystal structure of **5e** provides a very clear picture about the main features of the complex. First, the structure predicts two sets of *ortho*-F resonances (*syn* and *anti* with respect to the Fe-O-Fe moiety), both in the ratio of 2:1 (two of the C_6F_5 rings of each corrolato ligand are identical). Indeed, four different *ortho*-F resonances are clearly evident in Figure 3, and they are widely separated owing to the diamagnetic current effect of the neighboring corrole on the inner fluorine atoms. The sharp NMR resonances also indicate that the complex is diamagnetic, despite the relatively small Fe-O-Fe angle of 158°. This angle is significantly smaller than the optimal 180° for efficient coupling of the two d^4 iron cations through the bridging oxygen and of 170° obtained for

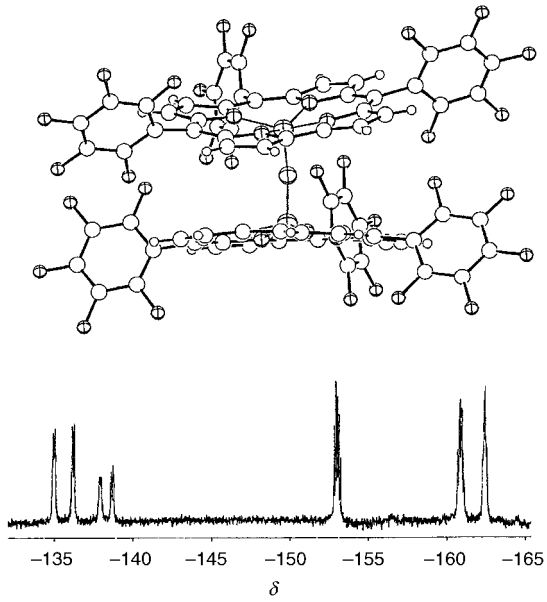

Figure 3. The X-ray structure [{Fe(tpfc)}$_2$O] (**5e**) and its ^{19}F NMR spectrum (25 °C, [D$_6$]benzene).

[{Fe(oec)}$_2$O] (**3c**). The most obvious explanation is that the structure of **5e** reflects a compromise between the electronically favored large Fe-O-Fe angle and consideration of the steric repulsion between the *meso*-C_6F_5 groups of the adjacent corroles (note also the staggered orientation of the latter). The alternative interpretation of the diamagnetism—a through space coupling of the macrocycles under an iron(III) corrole radical formalism—is not supported by the structure, since it would require a smaller separation of the two corroles and a more parallel orientation. It is worth mentioning at this point that in the crystal structures of the tpfc–metal complexes obtained so far we have not seen evidence for intermolecular interactions of the corroles, a dominant phenomenon in oec–metal complexes.[25]

The last iron corrole that was prepared is [Fe(tpfc)(NO)] (**5d**), from the reaction of [Fe(tpfc)Cl] (**5b**) with $NaNO_2$. This reaction is very simple to carry out,[8b] and **5d** appears to be a

0947-6539/01/0705-1044 $ 17.50+.50/0 *Chem. Eur. J.* **2001**, *7*, No. 5

very stable complex, even in aerobic solutions and unprotected from laboratory light. The characterization of **5d** and the assignment of the iron(III) oxidation state are also very easy, since it is the only mononuclear iron corrole that is expected to be diamagnetic. The comparison of Figure 4 and

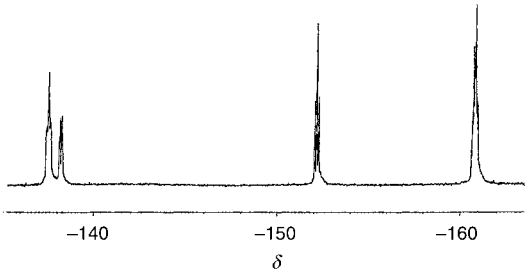

Figure 4. The ^{19}F NMR spectrum (25 °C, $CDCl_3$) of [Fe(tpfc)(NO)] (**5d**).

Figure 3 further serves to demonstrate that the basic features of the NMR spectra of **5d** and [{Fe(tpfc)}$_2$O] (**5e**) are similar, which may be expected since both are diamagnetic and contain pentacoordinated iron. Still, the above-mentioned large separation of the *ortho*-F resonances in **5e** is much smaller in **5d** due to the smaller differences of the two *ortho*-F sites in **5d**. Finally, the NO stretching frequency of 1790 cm^{-1} in **5d** is well within the range of linear nitrosyl complexes expected for iron(III),[26] and the comparison with 1767 cm^{-1} in [Fe(oec)(NO)] (**3a**) demonstrates that tpfc is significantly less electron-rich than oec.

Synthesis of the rhodium complexes of tris(pentafluorophenyl)corrole (H_3(tpfc) (4)): We have recently reported the synthesis and structural characterization of [Rh(tpfc)(PPh_3)] (**6a**),[18] obtained as the major product from the insertion of [$Rh_2(CO)_4Cl_2$] into **4**. The highly domed crystal structure of **6a** suggests that coordination of the rhodium by a larger phosphine might significantly change the steric environment and affect the cyclopropanation process. To test this proposal, we have now also prepared the rhodium complex with tricyclohexyl phosphine. In this case, the spontaneous oxidation of the initially obtained rhodium(I) corrole to rhodium(III) is much less efficient. This allowed the isolation of green dicarbonylrhodium(I) intermediates (see Scheme 3), which were also noted in the preparation of **6a**. According to MS the general structure is [Rh{H_2(tpfc)}$(CO)_2$] (**10a–c**), with the sharp resonances in the ^1H NMR spectra supporting the diamagnetic rhodium(I) oxidation state, and the observation of three NH singlets in the range $\delta = -4$ to -7 indicates that all three possible isomers are formed (Scheme 3).[27] The desired rhodium(III) complex, [Rh(tpfc){$P(C_6H_{11})_3$}] (**6b**), was obtained by stirring aerobic solutions of **10a–c** in the presence of excess $P(C_6H_{11})_3$.

Synthesis of the rhodium complex of a *N*-substituted corrole (11 → 12a, Scheme 4): We have recently reported that the *N*-substitution of **4** by benzyl bromide leads to two isomeric

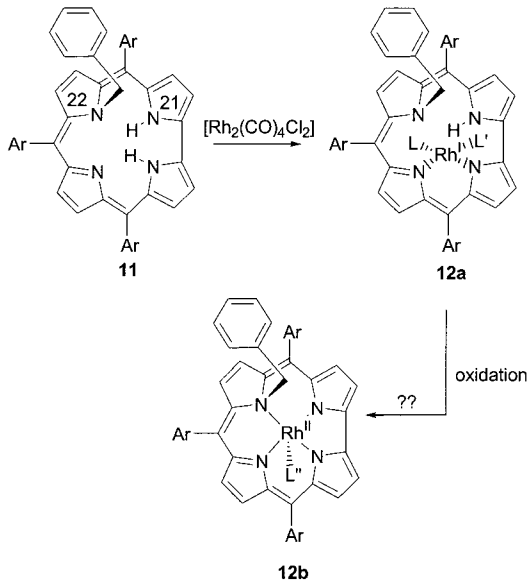

Scheme 4. Rhodium insertion into H_2(N^{22}-benz-tpfc) (**11**) to form **12a** (see Figure 5 for its X-ray structure) and its plausible oxidation product **12b** (L = CO, L′ = PPh_3, L″ = CO or PPh_3).

macrocycles, H_2(N^{21}-benz-tpfc) and H_2(N^{22}-benz-tpfc) (**11**);[6b] each of the isomers is chiral, can be separated into its enantiomers, and can still bind zinc(II).[20] We have now investigated the insertion of rhodium into racemic **11**, with [$Rh_2(CO)_4Cl_2$] as the metal carrier. After the reaction was complete (thin-layer chromatography (TLC)), the mixture was stirred in the presence of triphenyl phosphine and air. In contrast to the above-mentioned rhodium complexes of the nonsubstituted corrole, there was no spontaneous oxidation of the complex and the reaction product was isolated as a diamagnetic rhodium(I) complex (**12a**, Scheme 4). The general structure (from MS) of the product is [Rh{H(N^{22}-benz-tpfc)}(CO)(PPh_3)], which could correspond to any of the three possible isomers that differ only in the identity of the

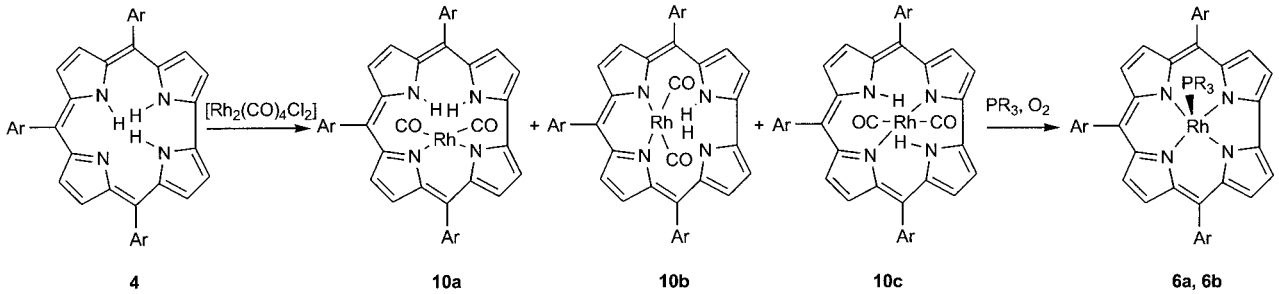

Scheme 3. Synthesis of the rhodium corroles (Ar = C_6F_5, R = C_6H_5 (**6a**) or C_6H_{11} (**6b**)).

nitrogen atoms bound to the metal or a mixture thereof.[28] However, according to the ^{1}H NMR spectrum only one particular isomer is formed, as indicated by the observation of only one set of free NH and benzylic protons at high field. Recrystallization from benzene/*n*-heptane allowed its X-ray crystallography characterization as **12a** (a single enantiomer thereof), as shown in Figure 5. The rhodium(I) ion is in a

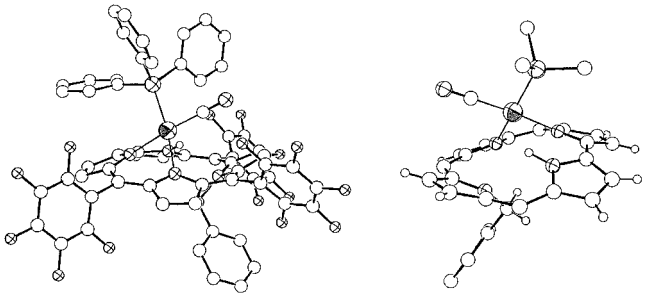

Figure 5. Full (hydrogen omitted) and partial views of the X-ray structure of **12a**.

square-planar coordination environment, with the metal bound to CO, PPh_3, the negatively charged N24 and the neutral N23 from the corrole. The N^{22}-benzyl moiety remains intact and is located at the opposite site of the corrole, and in the observed coordination mode and corrole conformation there probably is a weak N–H···N hydrogen-bonding interaction across the corrole ring. The complex is air-stable, but can be oxidized by a variety of mild oxidants (Br_2, NBS, I_2, NIS).[6b] The in situ oxidation by NIS was examined by NMR spectroscopy, upon which the diamagnetic resonances of **12a** were replaced by paramagnetic signals, an indication of oxidation to rhodium(II) (**12b**) and not rhodium(III).

Synthesis of the germanium, tin, and phosphorus corroles: The germanium(IV), tin(IV), and phosphorus(V) complexes of **4** were prepared in high yield by heating the corrole dissolved in pyridine or DMF together with excess $GeCl_4$, $SnCl_4$, and $POCl_3$ (no reaction with PCl_3), respectively. In all cases, the crude reaction mixture consisted of the desired metallation product, but as mixtures of chloro- and hydroxo-coordinated complexes (as observed by NMR spectroscopy). This problem was the least severe with tin, and pure [Sn(tpfc)Cl] (**8**) was obtained by extensive washing with concentrated HCl. The other two complexes were treated by flash chromatography, resulting in the hydroxo-coordinated products, [Ge(tpfc)OH] (**7b**) and [P(tpfc)$(OH)_2$] (**9**). In contrast to the hydrolytic lability of the chlorides, the coordinated hydroxide is not labile, as indicated by the lack of conversion into the chloro-coordinated complexes by treatment with concentrated HCl. The hydroxo protons are apparent in the NMR spectra and P–H couplings are observed for the β-pyrrole-H protons in **9** (high- and low-field parts, respectively, of Figure 6b). The electronic specta of all three complexes are very similar, with a sharp Soret band at 410–416 nm and two main *Q* bands at 550–600 nm (shown for **9** in Figure 6a, broken line).

Electrochemistry and spectroscopy of the germanium(IV), tin(IV), and phosphorus(V) corroles: The electrochemical investigations were performed for several purposes. First,

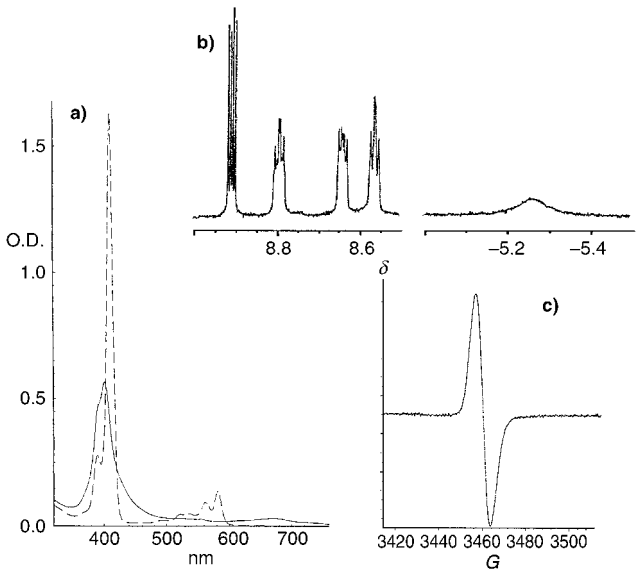

Figure 6. The UV/Vis (a, broken line) and ^{1}H NMR spectra (b, at 25 °C in [D_6]benzene) of P(tpfc)$(OH)_2$ (**9**) and the UV/Vis (a, full line) and EPR spectra (c, in CH_2Cl_2 at RT) of its corrole radical complex, obtained from the one-electron oxidation of **9** by the hexachloroantimonate salt of dibenzo-1,4-dioxin cation radical.

most existing data on corroles is about the metal complexes of the electron-rich H_3(oec),[3, 5] while the complexes of **4** present the other extreme of the most electron-poor corroles up to date. Our initial anticipation was that these differences will have a larger effect on the corrole than on the metal, thus allowing a better separation of the redox processes. Secondly, we wanted to determine the difference between the first oxidation and reduction potentials in [M(tpfc)L] (M represents a non-transition metal and L its axial ligand(s)), which provides the so-called electrochemical HOMO–LUMO gap of the corrole.[29] Among other things, this fundamental information is a very useful tool for distinguishing between metal- and corrole-centered redox processes. Spectroelectrochemistry was used in parallel with chemical oxidation to confirm that identical species were obtained, with the latter method used for preparing samples for EPR examination of the corrole radicals. All this information was later used in the analysis of the electrochemistry of the iron corroles with regard to the earlier mentioned metal versus corrole oxidation-site dilemma.

The half-wave potentials for the oxidation and reduction of all tpfc–metal complexes are compiled in Table 2, together with literature data for oec complexes. The first thing to note is the 0.53 V increase in the oxidation potential on moving from the electron-rich [Sn(oec)Cl] (**2a**) to the electron-poor [Sn(tpfc)Cl (**8**)] (entries 2 and 7). Secondly, the constant difference of 2.12 ± 0.02 V between the oxidation and reduction potentials in **8**, **7b**, and **9** (entries 7–9) clearly proves that in all cases only the corrole is involved in the redox processes. This is different from **2a**,[6] in which the metal is reduced at -1.46 V, much before the corrole's reduction is expected (a value of -1.94 V may be calculated from entries 1 and 2). Also, the HOMO–LUMO gap of 2.12 ± 0.02 V in [M(tpfc)L] may be compared with the value of 2.21 V for [Sn(oec)Ph]

0947-6539/01/0705-1046 $ 17.50+.50/0 *Chem. Eur. J.* **2001**, *7*, No. 5

Table 2. Half wave potentials (in V vs sce, in CH_2Cl_2 unless otherwise indicated) for oxidation and reduction of corrole metal complexes.

Entry	Metal (axial ligand)	Corrole	Cor/Cor$^{\bullet+}$	Cor/Cor$^{\bullet-}$	ΔE [V][a]	M^n/M^{n+1}	M^n/M^{n-1}	Reference
1	Sn^{IV}(Ph)	oec	0.47	−1.74	2.21			[6a]
2	Sn^{IV}(Cl)	oec	0.67				−1.46[b]	[6a]
3	Fe^{IV}(Cl)	oec	0.76				−0.08	[7a]
			0.79	−1.45	2.24		−0.07	[7a] (PhCN)
4	Fe^{IV}(Ph)	oec	0.43				−0.62	[7a]
			0.47	−1.98	2.45		−0.61	[7a] (PhCN)
5	Fe^{III}(pyr)	oec	1.03[e]			0.21	−1.04	[7a]
						0.28	−0.94	[7a] (pyridine)
6	Fe^{III}(NO)	oec	0.61	−1.92[e]	2.53		−0.41	[7b]
7	Sn^{IV}(Cl)	tpfc	1.20	−0.94	2.14			this work
8	Ge^{IV}(OH)	tpfc	1.13	−0.99	2.13			this work
9	$P^{V}(OH)_2$	tpfc	1.05	−1.05	2.10			this work
10	Fe^{IV}(Cl)	tpfc	1.24				0.44	this work
11	$Fe^{IV}(O)Fe^{IV}$	tpfc	1.25, 0.88				0.13	this work
12	$Fe^{III}(pyr)_2$	tpfc				0.74		this work[f]
13	Fe^{III}(NO)	tpfc	1.07				0.00	this work
14	$[Ar_3N]^{\bullet+}$[c]			1.11 for $[Ar_3N]^{\bullet+}/[Ar_3N]$				this work
15	dioxin[d]			1.41 for $[dioxin]^{\bullet+}/[dioxin]$				[10a]

[a] The difference in potentials for the first oxidation and the first reduction of the corrole. [b] Sn^{IV}/Sn^{II}. [c] Tris(4-bromophenyl)aminium hexachloroantimonate. [d] Dibenzo-1,4-dioxin. [e] Not assigned with full confidence. [f] There is also a irreversible reduction at −0.78 V.

(**2b**);[6, 12] these values are both in the range of 2.20 ± 0.15 V, which was obtained for a large range of metalloporphyrins.[29]

The oxidation potentials of **8**, **7b**, and **9** (entries 7–9) suggest that the commonly used and commercially available oxidant tris(4-bromophenyl)aminium hexachloroantimonate ($[Ar_3N]^{\bullet+}$) (entry 14) can only be used for the oxidation of **9**. However, with the radical of dibenzo-1,4-dioxin (as its hexachloroantimonate salt) all complexes should be oxidized (entry 15).[10a] This assumption was checked and found to be true and allowed the revelation of the spectral characteristics of all three corrole radical complexes, which appeared to be very similar. As can be seen in Figure 6a for **9**, there is an extremely large decrease in the intensity of the Soret band at 410 nm, with a slight blue-shift of the λ_{max} to 400 nm. Taking this phenomenon and the color change from red to green as criteria, the spectra of corrole and porphyrin radicals are similar. However, the characteristic appearances of new bands at above 600 nm in porphyrin radicals,[10] is much less pronounced in corrole radicals (this also holds for **2a** and **2b**).[6a]

The same methodology was also used for examination of the EPR spectra of the corrole radical complexes. Special attention was given to identify possible hyperfine splitting, which is expected if there is considerable spin density on the nitrogens or on the metal in the one-electron-oxidized germanium and phosphorus complexes. However, only singlets were obtained, with linewidths (halfwidth at half-hight) of 4, 20, and 6 G for **8**, **7b**, and **9** (Figure 6c), respectively. This suggests that the majority of the spin density is concentrated on the quaternary α-pyrrole carbons, similar to porphyrin radicals with an A_{1u} ground state.[10] This conclusion is further supported by most recent molecular orbital calculations of [Ga(tpfc)], which discloses the existence of two almost equal in energy highest occupied molecular orbitals, both of which have less spin density on the nitrogen atoms than in analogous porphyrins.[30] One outcome from the current investigations is that the spectral properties of corrole radicals are significantly less distinctive than that of porphyrin radicals. But, the constant difference between the first oxidation and reduction potentials of corroles remains a very useful tool for distinguishing between metal and corrole-centered oxidation, as demonstrated in the following section.

Electrochemistry of the iron corroles: The differences between the first oxidation and reduction potentials in the iron corroles are much smaller—0.8, 0.75, ~1.5, and 1.07 V in [Fe(tpfc)Cl] (**5b**), [{Fe(tpfc)}$_2$O] (**5e**), [Fe(tpfc)(py)$_2$] (**5c**), and [Fe(tpfc)NO] (**5d**), respectively (Table 2, entries 10–13)—than the electrochemical 2.1 V HOMO–LUMO gap of the corrole in the non-transition metal complexes of tpfc (**7**–**9**). This information readily enforces the conclusion that the metal is involved in at least one of the redox processes for all investigated iron corroles. With the oxidation potentials of 1.24 V for **5b** and 1.07 V for **5d** being in the range of 1.20–1.05 V obtained for **7**–**9**, the oxidations of **5b** and **5d** may be confidently assigned as corrole-centered. Accordingly, their reduction processes at 0.44 and 0.00 V must be metal-centered, that is, Fe^{IV}/Fe^{III} for **5b** and Fe^{III}/Fe^{II} for **5d** (reduction of the corrole in **5b** and **5d** should only be obtained at −0.86 and −1.03 V, respectively). Supporting evidence for an Fe^{IV}/Fe^{III} couple in **5b** is provided by its spectroelectrochemistry (Figure 7), which shows that its reduction leads to the appearance of the characteristics of iron(III) corroles such as **5a** and **5c**; a spectrum with a single red-shifted Soret band and *Q* bands at 534 and 710 nm is observed (this is accompanied by a color change from brown to red). A similar interpretation holds for the binuclear μ-oxo complex **5e**, for which two oxidation waves are obtained with $E_{1/2}$ of 1.25 and 0.88 V (Table 2, entry 11). The relatively low first oxidation potential is readily accounted for by a significant delocalization of the free electron in the singly oxidized product over both corrole rings of the binuclear complex. The 0.31 V shift to less positive potentials in **5e**

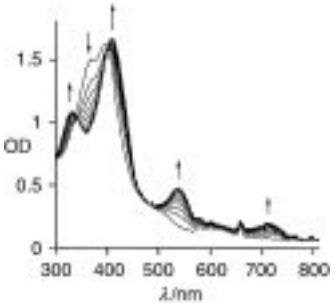

Figure 7. Spectral changes upon the reduction of [Fe(tpfc)Cl] (**5b**) at 200 mV (CH_2Cl_2, 0.1M TBAP).

($E_{1/2} = 0.13$V) relative to **5b** ($E_{1/2} = 0.44$ V) is consistent with metal reduction, as it may be attributed to a stronger π donation of the bridging oxygen than the chloride (a similar effect is seen in monomeric (chloro)iron(III) versus binuclear (μ-oxo)iron(III) porphyrin complexes).[29] Also important to note is that the reduction of **5e** is irreversible on the spectroelectrochemistry timescale, in which full conversion of **5e** to mononuclear iron(III) corrole is obtained.

The situation in the novel *trans*-bis-pyridine complex **5c** (indications for formation of the related [Fe(oec)$(py)_2$] are limited to low temperature and large excess of pyridine)[7] is more complex. While the oxidation potential of 0.74 V (Table 2, entry 12) for **5c** is much lower than the 1.05–1.20 V for corrole oxidation in the non-transition metal complexes (Table 2, entries 7–9), it is also significantly higher than the Fe^{III}/Fe^{IV} couples in **5b** and **5e** (0.44 and 0.12 V, respectively). Still, several indications are supportive of a metal-centered oxidation. First, spectroelectrochemical examination of **5c** at 1.0 V (not shown) reveals that upon oxidation the Soret band is shifted to a shorter wavelength, but without a large decrease in its intensity. Secondly, the much larger ligand-field stabilization energy in the low-spin iron(III) state of hexacoordinated **5c** than that found in the only weakly coordinated (by ClO_4^- or solvent molecules) iron(III) corrole, obtained by reduction of **5b**, should indeed lead to a relatively high Fe^{III}/Fe^{IV} potential for **5c**. Finally, addition of excess pyridine to a solution of **5b** in [D_6]benzene (for NMR spectroscopy) results in its immediate reduction to **5c**; this is in line with the much more positive reduction potential of an initially formed $[Fe^{IV}(tpfc)(py)_2]^+$ complex. The effect of pyridine ligation in **5c** is further amplified with the very strong-field and also highly non-innocent NO ligand in **5d**, as now the cor/cor$^{\bullet+}$ couple precedes the Fe^{III}/Fe^{IV} couple (in addition to the earlier mentioned indication for a corrole-centered oxidation, spectroscopic examination reveals a large decrease in the Soret band upon the oxidation of [Fe(tpfc)(NO)] by $[Ar_3N]^{\bullet+}$). In addition, it is the only complex for which the iron(II) oxidation state is accessible, as indicated by its highly positive Fe^{III}/Fe^{II} couple (0.00 V, entry 13 of Table 2). This effect is readily accounted for by considering the delocalization of the added electron into the π-accepting NO ligand.

The comparison between the (nitrosyl)iron(III) complexes **3a** and **5d** (entries 6 and 13) shows that despite the large dissimilarity of the corrole structures, the differences between the cor/cor$^{\bullet+}$ and the Fe^{III}/Fe^{II} redox couples are almost identical (1.02 vs. 1.07 V, respectively). A similar comparison of the differences between the cor/cor$^{\bullet+}$ and the Fe^{IV}/Fe^{III} couples in the (chloro)iron(IV) complexes of oec and tpfc (entries 3 and 10) also reveals their constancy, 0.84 and 0.80 V, respectively. Accordingly, the conclusion is that the quite excessive change in the structure of the corrole has no effect on the separation of the iron- and corrole-centered redox processes. It remains to be determined, by investigation of many other transition metal complexes of the oec and tpfc systems, whether this quite surprising phenomenon is general or specific to iron.

Cyclopropanation of styrene by carbenoids catalyzed by iron corroles: In our initial report, we used the iron(IV) corrole **3b** as a catalyst for the cyclopropanation of styrene by ethyl diazoacetate (EDA) and by the chiral carbenoid **13** (Scheme 5). We have now extended this research by the utilization of a variety of iron corroles in different oxidation and coordination states.

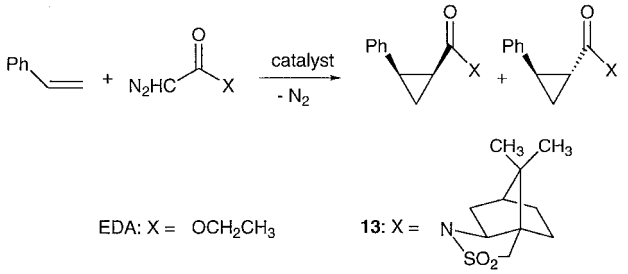

Scheme 5. Metallocorrole-catalyzed cyclopropanation of styrene by carbenoids.

Several results are immediately apparent from examination of Table 3. First, there is some solvent effect on the *anti*/*syn* product ratio, which is larger in CH_2Cl_2 than in benzene. Despite this advantage of the CH_2Cl_2, the iron(III) corroles were only checked in benzene because their oxidation to iron(IV) is more facile in CH_2Cl_2. With regard to the yield of the undesired coupling product of EDA (highly selective for maleate, with only traces of fumarate), the results in both solvents were similar. This side reaction could be diminished by using styrene as both solvent and reactant, and the *anti*/*syn* product ratio was identical to that in benzene. Secondly, the most significant result is the almost complete invariance of the product ratio for the different iron corroles. Regardless of the oxidation state of iron and its ligands, the product ratio was 1.5–1.6 in benzene and 1.9–2.3 in CH_2Cl_2. This suggests one common active intermediate, probably a metal carbene[31] and one common precursor for it. The fact that both iron(IV) and iron(III) complexes are catalytically active suggests that the common precursor is iron(III). This is especially true for the μ-oxo complex **5e**, which would otherwise expected to be inert, or at least provide very different selectivities owing to its quite different structure. Accordingly, we assume that the iron(IV) corroles are reduced by EDA, and that the lower reactivity of **5e** relative to the mononuclear **5b** is due to the more negative reduction potential of the former complex (Table 2, en-

0947-6539/01/0705-1048 $ 17.50+.50/0 *Chem. Eur. J.* **2001**, *7*, No. 5

Table 3. Cyclopropanation of styrene by ethyl diazoacetate (EDA) and by the chiral carbenoid **13** (entries 9–11), catalyzed by the various iron complexes of **4**.[a,c]

Entry	Catalyst	Solvent	Reaction time [h]	Yield of *anti*-[c] ester (or amide)	Yield of *syn*-[c] ester (or amide)	*anti*:*syn* ratio	Yield of cyclopropyl products	Yield of diethyl maleate
1	**5b**	CH_2Cl_2[b]	2.5	45%	20%	2.3	65%	33%
2	**5b**	benzene	2.5	38%	25%	1.5	63%	30%
3	**5b**	styrene	< 1.5	53%	36%	1.5	89%	9%
4	**5e**	benzene	7.5	38%	25%	1.5	63%	36%
5	**5a**	benzene	< 3	33%	21%	1.6	53%	43%
6	**5c**	benzene	4	31%	20%	1.6	51%	41%
7	**5c**	CH_2Cl_2	2.5	38%	20%	1.9	58%	38%
8	**5d**	CH_2Cl_2	5			no reaction		
9	**5b**	CH_2Cl_2[b,c]	24	25% *de* (1*S*,2*S*)	66% *de* (1*S*,2*R*)	0.9	41%	
10	**5b**	benzene[c,d]	24	28% *de* (1*S*,2*S*)	64% *de* (1*S*,2*R*)	0.6	78%	
11	**5a**	benzene[c,d]	24	32% *de* (1*S*,2*S*)	71% *de* (1*S*,2*R*)	0.6	76%	

[a] Catalyst/EDA/styrene = 1:500:5000, with 0.27–0.33 mM catalyst at room temperature (22–25 °C). [b] At 18 °C. [c] 100 equiv. **13** were added in one portion into a solution of 0.20–0.25 mM catalyst and 0.2–0.25 M of styrene. The identity of the major diastereomeric cyclopropyl amide is indicated in the parentheses. [d] 22 °C.

tries 10, 11). This proposal is reminiscent of previous observations with iron(III) porphyrins, in which EDA was found to act as a reducing agent for the metal to its divalent oxidation state.[32] Further support for one common intermediate is provided from the cyclopropanation of styrene by the much more sterically demanding and chiral carbenoid **13**, (Table 3, entries 9–11). The results with **5b** and **5a** were practically identical not only in the *anti*/*syn* product ratio, but also in the diastereomeric excesses (*de*'s) of each of the isomers. Finally, the only iron corrole which was not catalytically active is the nitrosyl complex **5d** (Table 3, entry 8), a fact that can be contributed to three reasons. It has a non-labile axial ligand, there is significant electron density withdrawal from the metal, and the nitrosyl ligand has a very strong *trans*-effect.

In principle, the hexa-coordinated complexes **5a** and **5c** may be considered as coordinatively saturated and accordingly expected not to be catalytically active. However, we have shown in the synthetic section that the axial ligands in both complexes are labile. In addition, in Table 4 we report the effect of adding pyridine to the reactions catalyzed by **5a** and **5b**. First, we noted that the addition of pyridine to either of the complexes resulted in identical UV/Vis spectral changes, with the final spectrum corresponding to that of **5c**. Inspection by NMR spectroscopy confirmed that **5c** is indeed formed under these conditions, through simple ligand exchange for **5b** (see also synthetic section) and by pyridine-induced reduction for **5a**.[33] In any case, the catalysis was only partially retarded by ten equivalents pyridine and there was almost no effect on the product ratio. Only with 200 equivalents of pyridine was the reactivity almost completely blocked, thus supporting the idea that only the pentacoordinated iron(III) corroles react with EDA. As for the presumable iron–carbene intermediate, the lack of any pronounced changes in the product ratio suggests that it is actually pentacoordinated (no *trans*-pyridine), which is also consistent with a strong *trans* effect of the carbene moiety.

Finally, we also attempted the characterization of the reactive intermediate—proposed to be a metal carbene in almost all related systems—by NMR spectroscopic examination of the reaction of several iron corroles with EDA in the absence of olefin. However, this proved to be a formidable task because of the very efficient dimerization of EDA to diethyl maleate under these conditions. Within the time required to record the first NMR spectrum, all EDA was consumed (transformed to diethyl maleate) and the unchanged catalyst was observed. Accordingly, we turned our attention to catalysis by rhodium corroles, for which this side reaction is much less pronounced.

Cyclopropanation of styrene by carbenoids catalyzed by rhodium corroles: In both the previous and the current investigations we have noted that the phosphine ligand of **6a** remains intact during catalysis. Accordingly, the binding and activation of the carbenoid and the interaction of the olefin with the presumed rhodium carbene must take place *trans* to the phosphine ligand. The previously obtained X-ray crystal

Table 4. Catalytic cyclopropanation of styrene in the presence of pyridine.[a]

	Catalyst	Solvent	Reaction time [h]	equiv of pyridine	*anti*-ester: *syn*-ester	Yield of cyclopropyl esters	Yield of diethyl maleate
1[b]	**5b**	CH_2Cl_2	2.5	0	2.3	65%	33%
2	**5b**	CH_2Cl_2	> 7	10	1.9	63%	28%
3	**5b**	CH_2Cl_2	24	200	1.8	3.4%	-
4[c]	**5a**	benzene	< 3	0	1.6	53%	43%
5	**5a**	benzene	4	10	1.6	50%	34%
6	**5a**	benzene	24	200	1.7	2.2%	–

[a] The same reaction conditions as in Table 3. [b] The same experiment as in entry 1 of Table 3. [c] The same experiment as in entry 5 of Table 3.

Table 5. Cyclopropanation of styrene by ethyl diazoacetate (EDA) and by the chiral carbenoid **13**, catalyzed by the rhodium(III) corroles with PPh_3 (**6a**) and $P(C_6H_{11})_3$ (**6b**) as axial ligands.[a,b]

Entry	Catalyst/ carbenoid	Solvent	Reaction time	Yield of *anti*- ester (or amide)	Yield of *syn*- ester (or amide)	*anti*:*syn* ratio	Yield of cyclopropyl products	Yield of diethyl maleate
1	**6a**/EDA	CH_2Cl_2	2 h	59%	30%	2.0	89%	<1%
2	**6a**/EDA	styrene	<1.5 h	62%	35%	1.8	97%	<1%
3	**6b**/EDA	CH_2Cl_2	1.5 h	61%	29%	2.1	90%	7%
4	**6a**/**13**	CH_2Cl_2	24 h	61% *de* (1*R*,2*R*)	9% *de* (1*S*,2*R*)	1.0	56%	
5	**6b**/**13**	CH_2Cl_2	24 h	18% *de* (1*R*,2*R*)	42% *de* (1*S*,2*R*)	0.7	6%	
6	**6b**/**13**	CH_2Cl_2	4 days	12% *de* (1*S*,2*S*)	44% *de* (1*S*,2*R*)	0.6	44%	

[a] Catalyst/carbenoid/styrene = 1:500:5000, with 0.27–0.33 mM catalyst at room temperature (22–25 °C). [b] 100 equivalents of **13** were added in one portion into a solution of 0.20–0.25 mM catalyst and 0.2–0.25 M of styrene. The identity of the major diastereomeric cyclopropyl amide is indicated in the parentheses.

structure of **6a** presents a highly domed corrole,[18] due to steric interactions of the triphenylphosphine with the *meso*-C_6F_5 substituents of the corrole. This suggests that different phosphine ligands might affect the selectivity in the cyclopropanation of styrene by carbenoids. To test this hypothesis, we have compared **6a** and the tricyclohexylphosphine coordinated complex **6b** as catalysts. Entries 1 and 2 of Table 5 show that **6a** is an excellent catalyst for the cyclopropanation of styrene by ethyl diazoacetate (EDA), with almost absolute selectivity (only traces of diethyl maleate are obtained). The effect of substituting PPh_3 by $P(C_6H_{11})_3$ (entry 3) is only small, with the main difference noted in the reduced selectivity (7% of diethyl maleate). However, the differences are amplified and quite pronounced for the reaction of styrene with the chiral and sterically demanding carbenoid **13** (entries 4–6). With **6a** as catalyst, the chemical yields are much larger, the *anti* and *syn* products are obtained in equimolar amounts, and the diastereomeric excess of the *anti*-cyclopropyl amide is much larger than that of the *cis* isomer. On the other hand, the chemical yields are largely reduced with **6b** as catalyst, the *syn*-cyclopropyl amide is the major product, obtained also with much larger *de* than in catalysis by **6a**. This proves that the axial ligand of the rhodium has a definite effect on the cyclopropanation process occurring *trans* to itself.

Based on these results, we prepared the rhodium complex (**11**) of the N^{22}-substituted corrole (Scheme 4). Since we have recently demonstrated the chirality and separation into enantiomers of this and other *N*-substituted corroles, we anticipated that such rhodium(II) complexes (**12b**, Scheme 4) could be very useful as asymmetric catalysts. The working hypothesis was that the coordinated PPh_3 will confine the reaction to the site *trans* to itself, while the chiral N-CH_2-Ph moiety will induce asymmetry. However, the X-ray structure of the rhodium insertion product, **12a** (Figure 5), revealed that it contains a rhodium(I) ion coordinated by only two corrole nitrogen atoms and that the *N*-substituent is very far from the square-planar coordination plane of the metal. These structural features are quite discouraging in terms of its utilization as catalyst for introducing asymmetry. Furthermore, although **12a** was found to be oxidizable by many mild oxidants, we could not fully characterize these paramagnetic products. Accordingly, only the racemic form of **11** was used in the current investigation, concentrating on the effect of in situ oxidation of the catalyst by NIS on the **12a**-catalyzed cyclopropanation of styrene by both EDA and **13**.

All four reactions summarized in Table 6 were continued until thin-layer and gas chromatography (TLC and GC) examinations indicated that the process was not proceeding any further. Although the total yields in the presence of NIS were lower than in its absence (comparing entries 1 and 3 with 2 and 4), this effect is contributed to the lower stability of the NIS-oxidized complex and not to its reactivity. At shorter reaction times (1.5 h with EDA and 18 h with **13**), the yields in the presence of NIS were actually much larger. Furthermore, the selectivities in the presence and absence of NIS were significantly different, especially in the reactions with **13**. Most important is that the diastereomeric excesses of both the *syn*- and the *anti*-cyclopropyl amides in entry 4 are much larger than of those in entry 3. Accordingly, we conclude that future work with *N*-substituted corroles as ligands for transition metals may eventually lead to very interesting chiral catalysts.

Table 6. Cyclopropanation of styrene by ethyl diazoacetate (EDA, entries 1–2)[a] and by the chiral carbenoid (**13**, entries 3–4),[b] catalyzed by the rhodium(I) complex **12a** (see Figure 5).

Entry	Solvent	Reaction time	Substrate	Additive	Yield of *anti*- ester (or amide)[b]	Yield of *syn*- ester (or amide)[b]	*anti*:*syn* ratio	Yield of cyclopropyl products	Yield of diethyl maleate
1	CH_2Cl_2	4 h	EDA	–	57%	36%	1.6	93%	5%
2	CH_2Cl_2	1.5 h	EDA	NIS	48%	31%	1.5	79%	<1%
3	CH_2Cl_2	4 days	**13**	–	57% *de* (1*R*,2*R*)	6% *de* (1*R*,2*S*)	1.0	50%	
4	CH_2Cl_2	18 h	**13**	NIS	73% *de* (1*R*,2*R*)	23% *de* (1*R*,2*S*)	0.8	36%	

[a] Catalyst/EDA/styrene = 1:500:5000 at about 17 °C, addition of EDA in one portion, 0.3 mM of catalyst were used. [b] 100 equivalents of diazo sultam were added in one portion into a solution of 0.23 mM catalyst and 0.23 M of styrene at about 19 °C. The identity of the major diastereomeric cyclopropyl amide is indicated in the parentheses.

0947-6539/01/0705-1050 $ 17.50+.50/0 *Chem. Eur. J.* **2001**, *7*, No. 5

Reaction of [Rh(tpfc)(PPh_3)] (6a) with EDA in the absence of olefins: In contrast to catalysis by the iron corroles, almost no dimerization products of EDA were obtained in the cyclopropanation of styrene catalyzed by rhodium(III) corrole (Table 5). This suggested that it might be possible to isolate reaction intermediates from the reaction of **6a** with EDA in the absence of olefins, a task that was not yet achieved with any of the highly efficient rhodium-based catalysts.[34] This proposal was first tested by in situ NMR experiments, which showed that the reaction between **6a** and EDA is very fast and that two new corrole complexes are formed in an about 2:1 ratio. The two products could be isolated by chromatography and were found by MS to be isomers of an addition product of **6a** and $CHCO_2Et$. Their NMR spectra shows that both complexes are diamagnetic, retain the PPh_3 ligand, and contain a $-CHCO_2Et$ moiety with the CH at very high field ($\delta = -3.5$ and -3.9). In addition, these signals appear as dd with distinct coupling constants of 13.4 and 2.0 Hz, reasonably accounted for by ^4J(P,H) and ^3J(Rh,H) couplings.[35] Spectral analysis and comparison to similar cobalt complexes[36] allowed the characterization of the two complexes (**14a** and **14b** in Scheme 6) as resulting from insertion of $CH(CO_2Et)$ into the Rh–N bonds of **6a**. This readily accounts for the observation of two isomers, since **6a** is of C_{2v} symmetry and contains two sets of Rh–N bonds. In the resulting structure the metal is pentacoordinated to PPh_3, the bridging carbon, and three of the corrole nitrogen atoms, with the rhodium(III) oxidation state balanced by two negatively charged corrole nitrogen atoms and the $^-CH(CO_2Et)N-$ moiety.

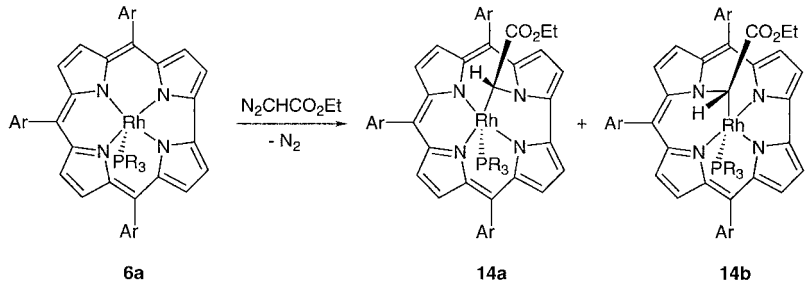

6a **14a** **14b**

Scheme 6. The reaction of **6a** with EDA in the absence of substrate.

The complexes **14a** and **14b** (Scheme 6) were stable enough for spectroscopic investigation, although within a few hours they gradually converted back into **6a**. Still, they were stable enough (they can be kept at $-20\,^\circ C$ for extended periods) for determining whether or not they are key intermediates in the cyclopropanation process. For this purpose, the reactions of **14a** and **14b** with styrene were investigated. When only styrene was added, their was no reaction. But, when both EDA and styrene were added to either of the isolated complexes, they did catalyze the cyclopropanation process. Furthermore, with both isomers, the *anti*/*syn* product ratios were identical and indistinguishable from that obtained with **6a** as catalyst. Accordingly, it may safely be concluded that **14a** and **14b** are not true reaction intermediates, but that the most important intermediate is probably a carbene complex, [*trans*-Rh=$CHCO_2Et$(tpfc)(PPh_3)] (see the effect of substituting PPh_3 by $P(C_6H_{11})_3$ at the *trans* position). This intermediate is in equilibrium with **14a** and **14b** and reacts with styrene to form the cyclopropanation products.

Conclusion

We report the first complexes of tris(pentafluorophenyl)corrole that contain the non-transtion metal ions germanium(IV), tin(IV), and phosphorus(V). Their electrochemistry reveals a constant 2.1 V electrochemical HOMO–LUMO gap, as well as the spectroscopic characteristics of corrole radical cations. This information was found to be highly valuable for assignment of the oxidation states of different iron–corrole complexes. One iron(IV) and one iron(III) corrole, as well as the rhodium(I) complex of an *N*-substituted corrole, were fully characterized by X-ray crystallography. Both the iron and the rhodium corroles are excellent catalysts for cyclopropanation of styrene, with the rhodium corroles displaying superior selectivities. From investigations of the effect of the oxidation state of the metal and its ligands, we conclude that with iron corroles the catalytically active form is iron(III), while all accesible oxidation states of rhodium are active. Two intermediates that are formed during catalysis with rhodium(III) were isolated, but shown not to be catalytically active. Future work will be devoted to the utilization of more crowded corroles, including metal complexes of *N*-substituted corroles.

Experimental Section

Physical methods: The NMR spectra were recorded on a Bruker AM200 spectrometer, operating at 200 MHz for ^{1}H and 188 MHz for ^{19}F. Chemical shifts in the ^{1}H NMR spectra are reported in ppm relative to residual hydrogens in the deuterated solvents: $\delta = 7.20$, 7.24 and 5.32 for benzene, chloroform and dichloromethane, respectively, and relative to $CFCl_3$ ($\delta = 0.00$) in the ^{19}F NMR spectra. Coupling constants *J* are reported in Hz. An HP 8452A diode array Spectrophotometer was used to record the electronic spectra. Gas chromatographic analysis was performed on a HP-5890 GC with a HP-5 capillary column and FID detector, linked to the HP Chem-Station (HP-3365). Chemical yields and *de*'s were reproducible within $\pm 2\%$ for multiple experiments. The redox potentials were determined by cyclic voltammetry (CV) at ambient temperatures on a home-made voltammograph, using CH_2Cl_2 solutions, 0.1 M in *n*-tetrabutylammonium perchlorate (TBAP, Fluka, recrystallized three times from absolute ethanol) and 10^{-3} M in substrate. The reference electrode was SCE, the scan rate 100 mV s^{-1} and the $E_{1/2}$ value for oxidation of ferrocene under these conditions was 0.465 V. The EPR spectra were recorded on a Bruker EMX 220 digital X-band radiospectrometer equipped with a Bruker ER 4121VT temperature control system operating within the temperature range of 100–700 K. Spectra processing and parameter calculations were performed with WIN-EPR software. Mass spectroscopy was performed on a Finnigan TSQ 70 instrument with isobutane as carrier gas, and IR spectra were recorded as KBr pellets on a FT-IR spectrometer Bruker Vector 22.

Materials: Benzene (Merck, thiophene free), for use in synthesis, was dried by distilling off a few mL. Benzene for use in catalysis was first washed with concentrated H_2SO_4 until the aqueous layer was colorless, followed by washing with water and aqueous NaOH, and distillation over CaH_2. Dichloromethane (Lab-Scan, HPLC grade) was either dried by distillation over CaH_2, or by passing through a column of basic alumina, with identical

results. DMF (Frutarom, analytical grade) was dried by distillation over CaH_2 at reduced pressure. Ethyl diazoacetate (EDA) (Fluka), $FeCl_2$ (anhydrous, Aldrich), $SnCl_2 \cdot 2H_2O$ (Merck), $POCl_3$ (Spectrum), $GeCl_4$ (Fluka), $[Rh_2(CO)_4(Cl)_2]$ (Aldrich, Strem), and the deuterated solvents (Aldrich and Cambridge Isotopes products) were used as received. Styrene (Riedel-de Haen) and nitrobenzene (Fluka) were filtered through a plug of basic alumina prior to their use in catalytic reactions, and the chiral carbenoid was prepared according to the published procedure.[37]

Synthetic methods: The synthetic details for the preparation of H_3(tpfc) (**4**) and H_2(N^{22}-benz-tpfc) (**11**) are provided in previous publications.[15, 20]

Insertion of iron into 4, for the synthesis of [Fe(tpfc)(OEt$_2$)$_2$] (5a), [Fe(tpfc)(py)$_2$] (5c), [{Fe(tpfc)}$_2$O] (5e), and [Fe(tpfc)Cl] (5b): All iron corroles were obtained by starting the synthesis with dissolving **4** (80 mg, 0.1 mmol) in dry DMF (30 mL) under N_2, and the addition of $FeCl_2$ (0.25 g, 2 mmol). The mixture was heated to reflux, and the process was followed by TLC (silica, *n*-hexane/CH_2Cl_2 2:1). After completing the iron insertion, the reaction mixture was cooled to 25 °C, and the solvent was evaporated. The resulting solid material was dissolved in diethyl ether, and chromatography over a short column (10 cm long, 2 cm diameter, with silica gel and diethyl ether as an eluent) was performed. The product, which was obtained after evaporation of the diethyl ether, was **5a**. The μ-oxo complex **5e** was obtained by recrystallization of **5a** from aerobic mixtures of acetonitrile and *n*-heptane, or diethyl ether and *n*-heptane. Pure **5c** was obtained by recrystallization of **5a** from diethyl ether/*n*-heptane mixtures in the presence of pyridine. For **5b**, the red-brown solid **5a** was dissolved in CH_2Cl_2, the resulting mixture was washed twice with HCl (7%), and finally with water. During the acidic washing, the color of the mixture changed from red-brown to deep brown. The solution was dried over Na_2SO_4, and the solvent was evaporated. Pure **5b** was obtained by recrystallization from benzene/*n*-heptane. The yields of all the reactions described herein were in the range of 90–95% for pure crystalline materials.

[Fe(tpfc)(OEt$_2$)$_2$] (5a): ^{1}H NMR (200 MHz, [D$_6$]benzene): $\delta = 19.71$ (s, 2H), 13.37 (s, 2H), −60.03 (s, 2H), −126.05 (s, 2H); ^{19}F NMR (188 MHz, [D$_6$]benzene): $\delta = -102.14$ (br s, 4F; *ortho*-F), −118.78 (br s, 2F; *ortho*-F), −149.38 (s, 1F; *para*-F), −150.95 (s, 2F; *para*-F), −156.29 (s, 2F; *meta*-F), −157.66 (s, 4F; *meta*-F); UV/Vis (diethylether): λ_{max} (relative ε) = 404 (100%), 546 nm (33%).

[Fe(tpfc)(py)$_2$] (5c): ^{1}H NMR (200 MHz, [D$_6$]benzene): $\delta = 56.52$ (br s, coordinated pyridine), 36.47 (s, coordinated pyridine), 3.21 (s, 2H), −61.05 (s, 2H), −65.80 (s, 2H), −134.56 (s, 2H); ^{19}F NMR (188 MHz, [D$_6$]benzene): $\delta = -102.89$ (br s, 4F; *ortho*-F), −119.45 (br s, 2F; *ortho*-F), −149.21 (s, 1F; *para*-F), −150.76 (s, 2F; *para*-F), −156.24 (s, 2F; *meta*-F), −157.45 (s, 4F; *meta*-F); UV/Vis (benzene:pyridine 50:1): λ_{max} ($\varepsilon \times 10^{-4}$): 412 (6.1), 548 (1.5); MS (DCI$^+$): *m*/*z*: 850 [*M*+H − 2pyridine]$^+$; MS (DCI$^-$): *m*/*z*: 849.1 [*M* − 2pyridine]$^-$; ^{1}H NMR (200 MHz, [D$_6$]benzene/[D$_5$]pyridine): $\delta = 2.14$ (s, 2H), −21.16 (s, 2H), −45.75 (s, 2H), −110.11 (s, 2H); ^{19}F NMR (188 MHz, [D$_6$]benzene/[D$_5$]pyridine): $\delta = -114.64$ (br s, 4F; *ortho*-F), −132.23 (br s, 2F; *ortho*-F), −153.64 (unresolved t, 1F; *para*-F), −154.72 (unresolved t, 2F; *para*-F), −161.87 (s, 6F; *meta*-F); ^{1}H NMR (200 MHz, $CDCl_3$): $\delta = 47.89$ (br s, coordinated pyridine), 3.47 (s, 2H), −63.93 (s, 2H), −65.06 (s, 2H), −128.85 (s, 2H); ^{19}F NMR (188 MHz, $CDCl_3$): $\delta = -101.41$ (br s, 4F; *ortho*-F), −116.65 (br s, 2F; *ortho*-F), −149.21 (s, 1F; *para*-F), −150.61 (s, 2F; *para*-F), −155.36 (s, 2F; *meta*-F), −157.04 (s, 4F; *meta*-F).

[{Fe(tpfc)}$_2$O] (5e): ^{1}H NMR (200 MHz, $CDCl_3$): $\delta = 7.07$ (d, ^3J(H,H) = 4.57 Hz, 4H), 6.79 (unresolved d, 4H), 6.50 (d, ^3J(H,H) = 5.01 Hz, 4H), 6.44 (d, ^3J(H,H) = 4.56 Hz, 4H); ^{19}F NMR (188 MHz, $CDCl_3$): $\delta = -135.01$ (d, ^3J(F,F) = 22.18 Hz, 2F; *ortho*-F), −136.21 (d, ^3J(F,F) = 22.94 Hz, 2F; *ortho*-F), −137.94 (d, ^3J(F,F) = 19.41 Hz, 1F; *ortho*-F), −138.70 (d, ^3J(F,F) = 23.88 Hz, 1F; *ortho*-F), −152.94 (m, 3F; *para*-F), −160.95 (m, 3F; *meta*-F), −162.32 (m, 4F; *meta*-F); UV/Vis (benzene): λ_{max} ($\varepsilon \times 10^{-4}$): 382 nm (11.4).

[Fe(tpfc)Cl] (5b): ^{1}H NMR (200 MHz, $CDCl_3$): $\delta = -2.84$ (s, 2H), −11.51 (s, 2H), −35.48 (s, 2H); ^{1}H NMR (200 MHz, [D$_6$]benzene): $\delta = -2.54$ (s, 2H), −3.08 (s, 2H), −12.07 (s, 2H), −33.58 (s, 2H); ^{19}F NMR (188 MHz, [D$_6$]benzene): $\delta = -159.286$, −160.370, −160.988, −164.136, −166.978, −169.860, −170.149; UV/Vis (CH_2Cl_2): λ_{max} ($\varepsilon \times 10^{-4}$) = 370 (4.3), 396 nm (4.6); MS (DCI$^+$): *m*/*z*: 849.9 [*M*+H − Cl]$^+$; MS (DCI$^-$): *m*/*z*: 847.6 [*M* − Cl]$^-$.

Synthesis of [Fe(tpfc)(NO)] (5d): Compound **5b** (20 mg, 23 μmol) was dissolved in CH_2Cl_2 (20 mL), followed by a saturated solution of $NaNO_2$ (2 mL). After 4 h of stirring at RT, the organic solvent was washed with water, dried over Na_2SO_4, and evaporated. Pure (NMR) deep-red material (14 mg, 70% yield) was obtained after column chromatography (silica, *n*-hexane/CH_2Cl_2 5:1). Final purification by recrystallization from benzene and *n*-heptane afforded (9 mg, 45% yield) of crystalline **5d**, which, however, did not refract well enough for X-ray crystallography. ^{1}H NMR (200 MHz, [D$_6$]benzene, RT): $\delta = 8.2$ (d, ^3J(H,H) = 4.5 Hz, 2H; β-pyrrole), 7.7 (d, ^3J(H,H) = 4.7 Hz, 2H; β-pyrrole), 7.5 (d, ^3J(H,H) = 4.8 Hz, 2H; β-pyrrole), 7.4 (d, ^3J(H,H) = 4.8 Hz, 2H; β-pyrrole); ^{19}F NMR (188 MHz, $CDCl_3$, RT): $\delta = -137.5$ (m, 4F; *ortho*-F), −138.2 (dd, ^3J(F,F) = 20.1 Hz, ^4J(F,F) = 5 Hz, 2F; *ortho*-F), −152.2 (t, ^3J(F,F) = 20.7 Hz, 3F; *para*-F), −160.8 (m, 6F; *meta*-F); IR (KBr): $\tilde{\nu} = 1790$ cm^{-1} (NO); UV/Vis (CH_2Cl_2): λ_{max} ($\varepsilon \times 10^{-4}$) = 378 (7.66), 534 nm (1.08); MS (DCI$^+$): *m*/*z* (%): 880.1 (30) [*M*+H]$^+$, 850 (100) [*M*+H − NO]$^+$; MS (DCI$^-$): *m*/*z* (%): 879.1 (10) [*M*]$^-$, 848.8 (100) [*M* − NO]$^-$.

Preparation of [Rh(tpfc)(PPh$_3$)] (6a): Compound **4** (50 mg, 0.06 mmol) was dissolved in dry benzene (20 mL) under N_2, and dry K_2CO_3 (0.87 g, 6.3 mmol), [{Rh(CO)$_2$Cl}$_2$] (70 mg, 0.18 mmol mg), and PPh_3 (82 mg, 0.31 mmol) were added to this mixture. The mixture was heated to reflux and the reaction was continued until TLC examinations (silica, *n*-hexane/CH_2Cl_2 2:1) indicated quantitative disappearance of the starting material (2.5 h). After cooling to RT, filtration, and solvent evaporation, several green products were obtained (TLC). During chromatography (silica gel, *n*-hexane/CH_2Cl_2 45:5), this mixture of rhodium(I) complexes converted spontaneously to the red complex, whose final purification was achieved by recrystallization from benzene and *n*-heptane. The yield of recrystallized **6a** from several syntheses was 52–58% (38–42 mg). ^{1}H NMR (200 MHz, $CDCl_3$): $\delta = 8.71$ (d, ^3J(H,H) = 4.71 Hz, 2H; β-pyrrole H), 8.41 (d, ^3J(H,H) = 4.86 Hz, 2H; β-pyrrole H), 8.24 (d, ^3J(H,H) = 4.76 Hz, 2H; β-pyrrole H), 8.14 (d, ^3J(H,H) = 4.42 Hz, 2H; β-pyrrole H), 7.02 (td, ^3J(H,H) = 7.76 Hz, ^4J(H,H) = 1.99 Hz, 3H; *para*-H of PPh_3), 6.67 (td, ^3J(H,H) = 7.98 Hz, ^4J(H,H) = 2.99 Hz, 6H; *meta*-H of PPh_3), 4.46 (dd, ^3J(H,H) = 12.51 Hz, ^4J(H,H) = 7.83 Hz, 6H; *ortho*-H of PPh_3); ^{19}F NMR (188 MHz, $CDCl_3$): $\delta = -137.61$ (m, 3F; *ortho*-F), −137.01 (dd, ^3J(F,F) = 22.44 Hz, ^4J(F,F) = 7.33 Hz, 2F; *ortho*-F), −138.37 (dd, ^3J(F,F) = 26.23 Hz, ^4J(F,F) = 8.74 Hz, 1F; *ortho*-F), −154.41 (t, ^3J(F,F) = 21.24 Hz, 3F; *para*-F), −162.57 (m, 3F; *meta*-F), −163.24 (m, 3F; *meta*-F); UV/Vis (CH_2Cl_2): λ_{max} ($\varepsilon \times 10^{-4}$) = 428 (6.6), 560 nm (1.6); MS (DCI$^+$): *m*/*z*: 1159.2 [*M*+H]$^+$; MS (DCI$^-$): *m*/*z*: 894.4 [*M* − PPh_3]$^-$.

Preparation of [Rh(tpfc){P(C$_6$H$_{11}$)$_3$}] (6b): The same procedure as described for **6a** was used, but with ten equivalents of tricyclohexyl phosphine instead of triphenylphosphine. In this case, chromatographic purification (silica gel, CH_2Cl_2/*n*-hexane 1:3) provided a green solid, which according to MS and ^{1}H and ^{19}F NMR spectroscopy is a mixture of different isomers of the diamagnetic rhodium(I) complexes, **10a–c** (MS (DCI$^+$): *m*/*z* (%): 955.3 (100) [*M*+H]$^+$, 896.3 (2) [*M*+H − 2H − 2(CO)]$^+$, 797.5 (25) [*M*+H − Rh − 2(CO)]$^+$; MS (DCI$^-$): *m*/*z* (%): 953.8 (100) [*M*]$^-$, 895.9 (5) [*M* − 2H − 2(CO)]$^-$, 796.1 (10) [*M* − Rh − 2(CO)]$^-$). Oxidation to rhodium(III) was achieved by dissolving the green solids in a mixture of CH_2Cl_2 and hexane, and stirring the solution for overnight in an open flask in the presence of excess P(C$_6$H$_{11}$)$_3$. Chromatography released some **4** (from demetallation), followed by red **6b**, which was recrystallized from CH_2Cl_2 and *n*-hexane. The yield from several syntheses was 43–45%. ^{1}H NMR (200 MHz, $CDCl_3$): $\delta = 8.85$ (d, ^3J(H,H) = 4.36 Hz, 2H; β-pyrrole H), 8.51 (d, ^3J(H,H) = 3.77 Hz, 2H; β-pyrrole H), 8.32 (d, ^3J(H,H) = 4.62 Hz, 2H; β-pyrrole H), 8.22 (d, ^3J(H,H) = 4.32 Hz, 2H; β-pyrrole H), 1.5 to −1 (m, 22H; unresolved ligand resonances); ^{19}F NMR (188 MHz, $CDCl_3$): $\delta = -137.53$ (m, 3F; *ortho*-F), −137.90 (dd, ^3J(F,F) = 24.1 Hz, ^4J(F,F) = 7.3 Hz, 2F; *ortho*-F), −138.51 (dd, ^3J(F,F) = 24.4 Hz, ^4J(F,F) = 7.1 Hz, 1F; *ortho*-F), −154.32 (t, ^3J(F,F) = 20.8 Hz, 3F; *para*-F), −162.49 (m, 3F; *meta*-F), −162.98 (m, 3F; *meta*-F); UV/Vis (CH_2Cl_2): λ_{max} ($\varepsilon \times 10^{-4}$) = 402 (6.8), 418 (sh), 558 (1.3), 582 nm (sh); MS (DCI$^+$): *m*/*z* (%): 1176.9 (100) [*M*+H]$^+$, 897.3 (62) [*M*+H − P(C$_6$H$_{11}$)$_3$]$^+$; MS (DCI$^-$): *m*/*z* (%): 895.8 (100) [*M* − P(C$_6$H$_{11}$)$_3$]$^-$.

Synthesis of [Rh{H(N^{22}-benz-tpfc)}(PPh$_3$)CO] (12a): PPh_3 (74 mg, 0.28 mmol), dry K_2CO_3 (0.77 g, 5.6 mmol), and dry NaOAc (1.15 g, 0.014 mol) were added to **11** (25 mg, 0.028 mmol) in dry benzene (30 mL). After heating the mixture to reflux under Ar, [{Rh(CO)$_2$Cl}$_2$] (108 mg, 0.28 mmol) was added in portions over 3 hours. After additional 2 hours heating under reflux, the reaction mixture was checked by TLC (silica, *n*-hexane/EtOAc 10:1), confirming that all starting material had

0947-6539/01/0705-1052 $ 17.50+.50/0 *Chem. Eur. J.* **2001**, *7*, No. 5

been consumed. The reaction mixture was cooled to 25 °C, filtered, and the solvent was evaporated. Purification of the material was achieved by column chromatography (silica gel, *n*-hexane/EtOAc 100:1, only one significant fraction), and a brilliant green solid material was obtained after evaporation of the solvent. The material was recrystallized from benzene and *n*-heptane. The average yield of pure **12a** from several syntheses was 55–60 %. ^{1}H NMR (200 MHz, $CDCl_3$): $\delta = 8.30$ (unresolved d, 1H; β-pyrrole H), 8.18 (d, $^3J(H,H) = 4.39$ Hz, 1H; β-pyrrole H), 8.02 (d, $^3J(H,H) = 4.45$ Hz, 1H; β-pyrrole H), 7.93 (m, 2H), 7.86 (unresolved d, 1H; β-pyrrole H), 7.76 (d, $^3J(H,H) = 4.25$ Hz, 1H; β-pyrrole H), 7.60 (d, $^3J(H,H) = 4.17$ Hz, 1H; β-pyrrole H), 6.77 (t, $^3J(H,H) = 6.30$ Hz, 3H; *para*-H, PPh_3), 6.58 (td, $^3J(H,H) = 7.28$ Hz, $^4J(H,H) = 2.56$ Hz, 6H; *meta*-H, PPh_3), 6.24 (t, $^3J(H,H) = 7.67$ Hz, 1H; *para*-H, N^{22}-aryl), 6.09 (t, $^3J(H,H) = 7.67$ Hz, 2H; *meta*-H, N^{22}-aryl), 5.82 (dd, $^3J(H,H) = 11.14$ Hz, $^4J(H,H) = 8.60$ Hz, 6H; *ortho*-H, PPh_3), 3.71 (d, $^3J(H,H) = 7.40$ Hz, 2H; *ortho*-H, N^{22}-aryl), 1.34 (s, 1H; NH), −4.60 (d, $^3J(H,H) = 15.02$ Hz, 1H; N^{22}-benzyl), −5.59 (d, $^3J(H,H) = 14.89$ Hz, 1H; N^{22}-benzyl); ^{19}F NMR (188 MHz, $CDCl_3$): $\delta = -137.21$ (dd, $^3J(F,F) = 25.00$ Hz, $^4J(F,F) = 7.33$ Hz, 1F; *ortho*-F), −137.67 (d, $^3J(F,F) = 24.82$ Hz, 1F; *ortho*-F), −138.59 (dd, $^3J(F,F) = 20.68$ Hz, $^4J(F,F) = 9.15$ Hz, 1F; *ortho*-F), −139.91 (m, 2F; *ortho*-F), −141.89 (dd, $^3J(F,F) = 23.50$ Hz, $^4J(F,F) = 5.64$ Hz, 1F; *ortho*-F), −152.95 (t, $^3J(F,F) = 22.00$ Hz, 1F; *para*-F), −153.33 (t, $^3J(F,F) = 21.24$ Hz, 1F; *para*-F), −153.84 (t, $^3J(F,F) = 21.81$ Hz, 1F; *para*-F), −161.64 (td, $^3J(F,F) = 22.94$ Hz, $^4J(F,F) = 6.96$ Hz, 1F; *meta*-F), −162.48 (m, 2F; *meta*-F), −163.32 (m, 3F; *meta*-F); UV/Vis (CH_2Cl_2): λ_{max} ($\varepsilon \times 10^{-4}$) = 466 (8.4), 614 nm (1.7). MS (DCI^+): *m*/*z* (%): 1279.1 (100) $[M+H]^+$, 1159 (12) $[M+H-C_7H_7-CO-H]^+$, 897.2 (16) $[M+H-C_7H_7-CO-H-PPh_3]^+$; MS ($DCI^-$): *m*/*z* (%): 1278.2 (100) $[M]^-$, 100 %).

Synthesis of [Sn(tpfc)Cl] (8): A solution of **4** (25 mg, 31.4 μmol) and $SnCl_2 \cdot 2H_2O$ (100 mg, 0.44 mmol) in DMF (3 mL) was heated to reflux for 30 minutes. The solvent was evaporated in a vacuum, and the residue was dissolved in CH_2Cl_2 and filtered. The filtrate was washed with concentrated HCl solution and evaporated. After recrystallization from hexane/CH_2Cl_2, **8** was obtained as dark violet crystals in 85 % yield (25.3 mg, 26.7 μmol). ^{1}H NMR (200 MHz, $CDCl_3$): $\delta = 9.4$ (d, $^3J(H,H) = 4.3$ Hz, 2H; β-pyrrole), 9.0 (d, $^3J(H,H) = 4.9$ Hz, 2H; β-pyrrole), 8.9 (m, 4H; β-pyrrole); ^{19}F NMR (188 MHz, $CDCl_3$): $\delta = -136.5$ (dd, $^3J(F,F) = 22.6$ Hz, $^4J(F,F) = 11.0$ Hz, 2F; *ortho*-F), −136.6 (dd, $^3J(F,F) = 22.6$ Hz, $^4J(F,F) = 9.0$ Hz, 1F; *ortho*-F), −137.9 (dd, $^3J(F,F) = 22.6$ Hz, $^4J(F,F) = 9.0$ Hz, 1F; *ortho*-F), −138.2 (dd, $^3J(F,F) = 24.9$ Hz, $^4J(F,F) = 9.0$ Hz, 2F; *ortho*-F), −152.0 (t, $^3J(F,F) = 22.6$ Hz, 2F; *para*-F), −152.2 (t, $^3J(F,F) = 22.6$ Hz, 1F; *para*-F), −161.7 (m, 6F; *meta*-F); UV/Vis (CH_2Cl_2): λ_{max} ($\varepsilon \times 10^{-4}$): 396 (4.7), 416 (21.5), 566 (1.5), 588 nm (1.4); MS (DCI^+): *m*/*z* (%): 949.0 (100) $[M+H]^+$, 912.9 (20) $[M+H-Cl]^+$.

Synthesis of [P(tpfc)(OH)$_2$] (9): $POCl_3$ (400 μL, 4.3 mmol) was added in one portion to a boiling solution of **4** (40 mg, 50.2 μmol) in pyridine (4 mL) under N_2. After 30 minutes of heating under reflux the solvent was evaporated, and the residue was dissolved in CH_2Cl_2 and filtered. The filtrate was washed with HCl (0.1M), dried, and evaporated. The residue was passed through a column of silica with CH_2Cl_2 as eluent, to remove excess of inorganic salts. After recrystallization from hexane/CH_2Cl_2, **9** was obtained as red crystals in 87 % yield (37.5 mg, 43.7 μmol). ^{1}H NMR (400 MHz, [D$_6$]benzene): $\delta = 8.9$ (dd, $^3J(H,H) = 4.5$ Hz, $^4J(P,H) = 2.4$ Hz, 2H; β-pyrrole H), 8.8 (dd, $^3J(H,H) = 4.7$ Hz, $^4J(P,H) = 2.1$ Hz, 2H; β-pyrrole H), 8.7 (dd, $^3J(H,H) = 4.0$ Hz, $^4J(P,H) = 2.7$ Hz, 2H; β-pyrrole H), 8.6 (dd, $^3J(H,H) = 4.4$ Hz, $^4J(P,H) = 3.3$ Hz, 2H; β-pyrrole H), −5.3 (br s, 2H; OH); ^{19}F NMR (188 MHz, [D$_6$]benzene): $\delta = -137.60$ (dd, $^3J(F,F) = 24.6$ Hz, $^4J = 8.5$ Hz, 6F; *ortho*-F), −151.7 (t, $^3J(F,F) = 21.2$, 1F; *para*-F), −151.8 (t, $^3J(F,F) = 21.8$, 2F; *para*-F), −161.5 (m, 6F; *meta*-F); UV/Vis (CH_2Cl_2): λ_{max} ($\varepsilon \times 10^{-4}$): 388 (10.3), 410 (45.3), 560 (5.2), 582 nm (6.6); MS (DCI^-): *m*/*z* (%): 858.1 (20) $[M]^-$, 912.9 (100) $[M-H_2O]^-$.

Synthesis of [Ge(tpfc)Cl] (7a): $GeCl_4$ (200 μL, 1.7 mmol) was added in one portion to a boiling solution of **4** (20 mg, 25.1 μmol) in DMF (3 mL). After 30 minutes of heating under reflux the solvent was evaporated, and the residue was dissolved in CH_2Cl_2 and filtered. The filtrate was washed with HCl (0.1M), dried and evaporated. After recrystallization from benzene/heptane, **7a** was obtained as dark violet crystals in 90 % yield (20.4 mg, 22.6 μmol). ^{1}H NMR (200 MHz, $CDCl_3$): $\delta = 9.6$ (d, $^3J(H,H) = 3.9$ Hz, 2H; β-pyrrole H), 9.1 (m, 4H; β-pyrrole H), 8.9 (d, $^3J(H,H) = 4.1$ Hz, 2H; β-pyrrole H); ^{19}F NMR (188 MHz, $CDCl_3$): $\delta = -136.4$ (d, $^3J(F,F) = 25.0$ Hz, 3F; *ortho*-F) −137.7 (d, $^3J(F,F) = 24.0$ Hz, 3F; *ortho*-F), −151.80 (t, $^3J(F,F) = 20.0$ Hz, 3F; *para*-F), −161.3 (m, 6F; *para*-F); UV/Vis (CH_2Cl_2): $\lambda_{max} = (\varepsilon \times 10^{-4})$: 394 (6.0), 410 (17.1), 562 (1.9), 576 nm (2.1); MS (DCI^+): *m*/*z* (%): 903.0 (100) $[M+H]^+$, 867.0 (65) $[M+H-Cl]^+$.

Synthesis of [Ge(tpfc)OH] (7b): Compound **7a** (20 mg, 22.2 μmol) was passed through a column of silica with CH_2Cl_2 as eluent. After recrystallization from hexane/CH_2Cl_2 **7b** was obtained as red crystals in 83 % yield (14.7 mg, 16.6 μmol). ^{1}H NMR (200 MHz, [D$_6$]benzene): $\delta = 9.2$ (d, $^3J(H,H) = 4.4$ Hz, 2H; β-pyrrole H), 8.8 (d, $^3J(H,H) = 4.8$ Hz, 2H; β-pyrrole H), 8.6 (m, 4H; β-pyrrole H), −5.1 (br s, 1H; OH); ^{19}F NMR (188 MHz, [D$_6$]benzene): $\delta = -137.3$ (dd, $^3J(F,F) = 21.0$ Hz, $^4J(F,F) = 8.0$ Hz, 2F; *ortho*-F), −1337.5 (dd, $^3J(F,F) = 25.0$ Hz, $^4J(F,F) = 8.0$ Hz, 1F; *ortho*-F), −138.3 (dd, $^3J(F,F) = 25.2$ Hz, $^4J(F,F) = 8.0$ Hz, 1F; *ortho*-F), −138.5 (dd, $^3J(F,F) = 23.9$ Hz, $^4J(F,F) = 8.0$ Hz, 2F; *ortho*-F), −151.9 (t, $^3J(F,F) = 22.5$ Hz, 1F; *para*-F), −152.0 (t, $^3J(F,F) = 21.2$ Hz, 2F; *para*-F), −161.3 (m, 3F; *meta*-F), −162.0 (m, 3F; *meta*-F); UV/Vis (CH_2Cl_2): λ_{max} ($\varepsilon \times 10^{-4}$): 386 (3.8), 410 (20.7), 560 (1.7), 576 nm (1.5); MS (DCI^+): *m*/*z* (%): 883.4 (80) $[M-H]^+$, 867.0 (100) $[M-OH]^+$; MS (DCI^-): *m*/*z* (%): 884.2 (100) $[M]^-$.

X-ray crystallography of 5e, 5c, and 12a: X-ray quality crystals of these complexes were obtained by slow recrystallization from mixtures of acetonitrile/*n*-heptane, diethyl ether/*n*-heptane (in the presence of pyridine), and benzene/*n*-heptane, respectively. The diffraction data were collected on a Nonius KappaCCD diffractometer with $Mo_{K\alpha}$ ($\lambda = 0.7107$ Å) radiation and reduced to intensities by DENZO.[38] The crystal structures were solved by a combination of Patterson and direct methods (DIRDIF-96 and SIR-92)[39, 40] and refined by full-matrix least-squares on F^2 (SHELXL-97).[41] All non-hydrogen atoms were treated anisotropically (expect for atoms of the partly disordered molecules of the respective crystallization solvents, which were refined in an isotropic manner). The hydrogen atoms were located in calculated positions to correspond to standard bond lengths and angles, the methyl substituents were treated as rigid groups. The small size of the crystals and their solvent content dictated low-temperature measurements in order to enhance their diffraction. Crystallographic data (excluding structure factors) for the structures reported in this paper have been deposited with the Cambridge Crystallographic Data Centre as supplementary publication no. CCDC-147594 (**5e**), CCDC-147594 (**5c**), and CCDC-147596 (**12a**). Copies of the data can be obtained free of charge on application to CCDC, 12 Union Road, Cambridge CB2 1EZ, UK (fax: (+44) 1223-336-033; e-mail: deposit@ccdc.cam.ac.uk). The selected crystallographic data for the analyzed structures are:

[{Fe(tpfc)}$_2$O] (5e): $(C_{37}H_8F_{15}FeN_4)_2O \cdot C_7H_{16}$, $M_r = 1814.85$, orthorhombic, space group *Pbca*, $a = 13.100(1)$, $b = 30.512(1)$, $c = 35.631(1)$ Å, $V = 14242.0(5)$ Å^3, $Z = 8$, $T = 110$ K, $\rho_{calcd} = 1.693$ g cm^{-3}, μ ($Mo_{K\alpha}$) = 0.54 mm^{-1}, 12628 unique reflections, $R_1 = 0.068$ for 7532 observed reflections with $F_o > 4\sigma(F_o)$, $R_1 = 0.134$ ($wR_2 = 0.244$) for all unique data, $|\Delta\rho| \leq 1.48$ e Å^{-3}. One mole of partly disordered *n*-heptane solvent was included in the crystal lattice.

[Fe(tpfc)(py)$_2$] (5c): $C_{47}H_{18}F_{15}FeN_6 \cdot 1.5(C_5H_5N)$, $M_r = 1126.17$, monoclinic, space group *C*2/*c*, $a = 40.725(2)$, $b = 8.672(3)$, $c = 26.896(1)$ Å, $\beta = 97.96(1)°$, $V = 9407.2(7)$ Å^3, $Z = 8$, $T = 115$ K, $\rho_{calcd} = 1.590$ g cm^{-3}, μ ($Mo_{K\alpha}$) = 0.43 mm^{-1}, 8736 unique reflections, $R_1 = 0.101$ for 6118 observed reflections with $F_o > 4\sigma(F_o)$, $R_1 = 0.140$ ($wR_2 = 0.276$) for all unique data, $|\Delta\rho| \leq 0.85$ e Å^{-3}. The precision of this determination was affected by structural disorder of some fragments of the structure. Thus, the central C_6F_5 ring revealed partial orientational disorder, which could not be resolved. The pyridine molecules contained in the crystal lattice (1.5 molecules per asymmetric unit) appear severely disordered as well.

[Rh{H(N^{22}-benz-tpfc)}(CO)(PPh$_3$)] (12a): $C_{63}H_{31}F_{15}N_4OPRh \cdot 0.5(C_6H_6)$, $M_r = 1317.85$, monoclinic, space group *C*2/*c*, $a = 34.711(1)$, $b = 13.143(1)$, $c = 26.951(1)$ Å, $\beta = 117.81(1)°$, $V = 10874.8(7)$ Å^3, $Z = 8$, $T = 115$ K, $\rho_{calcd} = 1.610$ g cm^{-3}, μ ($Mo_{K\alpha}$) = 0.45 mm^{-1}, 9718 unique reflections, $R_1 = 0.068$ for 5288 observed reflections with $F_o > 4\sigma(F_o)$, $R_1 = 0.116$ ($wR_2 = 0.169$) for all unique data, $|\Delta\rho| \leq 1.08$ e Å^{-3}. One molecule of the benzene solvent was located on a twofold rotation axis.

Spectroscopy of metallocorrole cation radicals: Samples for ESR spectroscopy were prepared by putting the solid metallocorrole (2 mg, 2.3 μmol) together with the hexachloroantimonate salt of dibenzo-1,4-dioxin cation radical (0.5 mg, 1 μmol) in a quartz ESR cuvette and degassing that tube by vacuum. Dry and degassed CH_2Cl_2 (0.3 mL) was added by vacuum transfer

into the ESR tube cooled with liquid nitrogen. The tube was sealed and kept frozen until used for measurements. The g values (CH_2Cl_2 at room temperature) of **7b**, **8**, and **9** were 2.0146, 2.0125, and 2.0136, with linewidths of 20, 4, and 6 G, respectively.

General procedure for the catalytic cyclopropanation of styrene by EDA: The catalyst (0.4 – 0.7 μmol) was dissolved in CH_2Cl_2 or benzene for the preparation of a 0.27 – 0.33 mM solution of the catalyst. Styrene (2 – 3.5 mmol), nitrobenzene (as an internal standard; 40 – 70 μmol), and EDA (0.2 – 0.35 mmol) were added to this solution under argon. In most cases, the mixture was stirred at room temperature until no more EDA was detected by TLC. Such reaction mixtures were checked by GC without any workup procedures for determination of the yield of *syn*- and *anti*-cyclopropyl esters and the yield of diethyl maleate (no fumarate was obtained in any of the metallocorrole-catalyzed cyclopropanation reactions). In the cases of incomplete reactions, the residual EDA was first consumed by washing the reaction mixture with a HCl (2 M), followed by washing with saturated solution of $NaHCO_3$, water, and drying. This workup procedure was necessary for preventing the thermal reaction between styrene and EDA in the GC injector. The GC retention times of nitrobenzene, diethyl maleate, diethyl fumarate, the *syn*-, and *anti*-cyclopropyl ester are 6.95, 8.50, 8.75, 12.81, and 13.50 min, respectively, under the following conditions: initial (3 min) and final temperatures of 80 and 200 °C, respectively, heating rate of 10 °C min^{-1}, at 7 psi. The identification of the *cis*- and *trans*-cyclopropyl ester isomers was based on comparison with the results obtained with [Fe(tpfp)Cl] as catalyst,[33] and that of the other materials by injection of commercially available substrates.

General procedure for the catalytic cyclopropanation of styrene by the chiral carbenoid 13: The catalyst (0.4 – 0.7 μmol) was dissolved in CH_2Cl_2 for the preparation of a 0.25 – 0.30 mM solution of catalyst. Styrene (0.4 mmol), internal standard (1 – 1.5 mg, 4 – 6 mmol), and **13** (40 – 70 μmol) were added to this solution under argon. The mixture was stirred at room temperature for the time indicated in Tables 3, 5 and 6. Prior to determination of the cyclopropanation results by GC, excess styrene (elutes with hexane) was separated from all other materials (eluted with CH_2Cl_2) by chromatography on silica in order to prevent the thermal reaction between carbenoid and styrene in the GC detector. The GC retention times (isothermal, 210 °C, 20 psi) of the *syn*-diastereoisomers are 23.5 and 26.3 min for (*R*,*S*) and (*S*,*R*), respectively, and 30.3 and 34.3 min for the (*R*,*R*) and (*S*,*S*) *anti*-diastereoisomers, respectively. The identification of the isomers was based on comparison with the results obtained with [$Rh_2(OAc)_4$] as catalyst.[38]

Acknowledgement

This research was supported in part by "The Fund for the Promotion of Research at the Technion" (ZG) and the Israel Science Foundation administered by the Israel National Academy of Sciences and Humanities (IG).

[1] a) J. L. Sessler, S. J. Weghorn, *Expanded*, *Contracted*, *and Isomeric Porphyrins*, Pergamon, Oxford, **1997**, pp. 11 – 125; b) A. Jasat, D. Dolphin, *Chem. Rev.* **1997**, *97*, 2267; c) E. Vogel, *J. Heterocycl. Chem.* **1996**, *33*, 1461.

[2] a) A. W. Johnson, I. T. Kay, *Proc. Chem. Soc.* **1964**, 89; b) S. Licoccia, R. Paolesse, *Struct. Bonding* **1995**, *84*, 71 – 133.

[3] a) Y. Murakami, Y. Matsuda, S. Yamada, *J. Chem. Soc. Dalton Trans.* **1981**, 855; b) Y. Matsuda, S. Yamada, K. Murakami, *Inorg. Chem.* **1992**, *31*, 2305.

[4] E. Vogel, S. Will, A. S. Tilling, L. Neumann, J. Lex, E. Bill, A. X. Trautwein, K. Wieghardt, *Angew. Chem.* **1994**, *106*, 771; *Angew. Chem. Int. Ed. Engl.* **1994**, *33*, 731.

[5] S. Will, J. Lex, E. Vogel, V. A. Adamian, E. V. Caemelbecke, K. M. Kadish, *Inorg. Chem.* **1996**, *35*, 5577.

[6] a) K. M. Kadish, S. Will, V. A. Adamian, B. Walther, C. Erben, Z. Ou, N. Guo, E. Vogel, *Inorg. Chem.* **1998**, *37*, 4573; b) Abbreviations: oep; the dianion of 2,3,7,8,12,13,17,18-octaethylporphyrin, oec; the trianion of 2,3,7,8,12,13,17,18-octaethylcorrole, tpfc; the trianion of 5,15,20-tris(pentafluorophenyl)corrole, N^{21}-benz-tpfc and N^{22}-benz-tpfc; the dianions of N^{21}- and N^{22}-benzyl-5,15,20-tris(pentafluorophenyl)corrole, respectively, NBS; *N*-bromo-succinimide, NIS; *N*-iodo-succinimide, EDA; ethyl diazoacetate.

[7] a) E. V. Caemelbecke, S. Will, M. Autret, V. A. Adamian, J. Lex, J.-P. Gisselbrecht, M. Gross, E. Vogel, K. M. Kadish, *Inorg. Chem.* **1996**, *35*, 185; b) M. Autret, S. Will, E. V. Caemelbecke, J. Lex, J.-P. Gisselbrecht, M. Gross, E. Vogel, K. M. Kadish, *J. Am. Chem. Soc.* **1994**, *116*, 9141.

[8] a) S. Will, J. Lex, E. Vogel, H. Schmickler, J. P. Gisselbrecht, C. Haubtmann, M. Bernard, M. Gross, *Angew. Chem.* **1997**, *109*, 367; *Angew. Chem. Int. Ed. Eng.* **1997**, *36*, 357; b) K. M. Kadish, V. A. Adamian, E. V. Caemelbecke, E. Gueletii, S. Will, C. Erben. E. Vogel, *J. Am. Chem. Soc.* **1998**, *120*, 11 986; for an isolated Mn^{III} center in the complex with H_3 (tpfc) (**4**), see: J. Bendix, G. Golubkov, H. B. Gray, Z. Gross, *Chem. Commun.* **2000**, 1957.

[9] a) S. Cai, F. A. Walker, S. Licoccia,, *Inorg. Chem.* **2000**, *39*, 3466; b) S. Licoccia, E. Morgante, R. Paolesse, F. Polizio, M. O. Senge, E. Tondello, T. Boschi, *Inorg. Chem.* **1997**, *36*, 1564.

[10] a) C. M. Barzilay, S. A. Sibilia, T. G. Spiro, Z. Gross, *Chem. Eur. J.* **1995**, *1*, 222; b) N. Ehlinger, W. R. Scheidt, *Inorg. Chem.* **1999**, *38*, 1316.

[11] R. Paolesse, S. Licoccia, T. Boschi, *Inorg. Chem. Acta.* **1990**, *178*, 9; b) R. Paolesse, S. Licoccia, T. Boschi, R. G. Khoury, K. M. Smith, *Chem. Commun.* **1998**, 1119.

[12] After this work was completed, we have learned that the preparation of As, Sb, and Bi complexes of H_3(oec) and their electrochemistry have been reported in a preliminary form, in: C. Erben, S. Will, K. M. Kadish in *The Porphyrin Handbook*, *Vol.* 2 (Eds.: K. M. Kadish, K. M. Smith, R. Guilard), Academic Press, **2000**, p. 233.

[13] Z. Gross, L. Simkhovich, N. Galili, *Chem. Commun.* **1999**, 599.

[14] R. Paolesse, S. Licoccia, G. Bandoli, A. Dolmella, T. Boschi, *Inorg. Chem.* **1994**, *33*, 1171; b) R. Paolesse, E. Tassoni, S. Licoccia, M. Pasi, T. Boschi, *Inorg. Chem. Acta.* **1996**, *241*, 55; c) S. Neya, K. Ohyama, N. Funasaki, *Tetrahedron Lett.* **1997**, *38*, 4113; d) R. Paolesse, L. Jaquinod, D. J. Nurco, S. Mini, F. Sagone, T. Boschi, K. M. Smith, *Chem. Commun.* **1999**, 1307.

[15] Z. Gross, N. Galili, I. Saltsman, *Angew. Chem.* **1999**, *111*, 1530; *Angew. Chem. Int. Ed.* **1999**, *38*, 1427; b) Z. Gross, N. Galili, L. Simkhovich, I. Saltsman, M. Botoshansky, D. Bläser, K. Boese, I. Goldberg, *Org. Lett.* **1999**, *1*, 599.

[16] a) H_3(tpfc) is now commercially available from Strem Chemicals (Illinois); b) N. Galili-Nachshon, L. Simkhovich, Z. Gross, I. Saltsman (Technion R & D), IPC C07D487/22 (WO 00/18771, 6. 4. 2000).

[17] Z. Gross, G. Golubkov, L. Simkhovich, *Angew. Chem.* **2000**, *112*, 4211; *Angew. Chem. Int. Ed.* **2000**, *39*, 4045.

[18] L. Simkhovich, N. Galili, I. Saltsman, I. Goldberg, Z. Gross, *Inorg. Chem.* **2000**, *39*, 2704.

[19] A. E. Meier-Callahan, H. B. Gray, Z. Gross, *Inorg. Chem.* **2000**, 3605.

[20] Z. Gross, N. Galili, *Angew. Chem.* **1999**, *111*, 2536; *Angew. Chem. Int. Ed.* **1999**, *38*, 2366.

[21] M. J. M. Nesset, S. Cai, T. K. Shokhireva, N. V. Shokhirev, S. E. Jacobson, K. Jayaraj, A. Gold, F. A. Walker, *Inorg. Chem.* **2000**, *39*, 532, and references therein.

[22] O. Q. Munro, J. A. Serth-Guzzo, I. Turowska-Tyrk, K. Mohanrao, T. K. Shokhireva, F. A. Walker, P. G. Debrunner, W. R. Scheidt, *J. Am. Chem. Soc.* **1999**, *121*, 11 144, and references therein.

[23] G. N. La Mar, F. A. Walker, in *The Porphyrins*, *Vol. IV* (Ed.: D. Dolphin), Academic Press, New York, **1979**, p. 61.

[24] Further characterization of these interesting iron(III) corroles by additional magnetic and spectroscopic methods is in process and will be published soon.

[25] See references [4, 7, 12].

[26] D. M. P. Mingos, D. J. Sherman *Adv. Inorg. Chem.* **1989**, *34*, 293.

[27] For previous indications for such rhodium(I) complexes, see: a) R. Grigg, J. Trocha-Grimshaw, V. Viswanatha, *Tetrahedron Lett.* **1976**, 289; b) A. M. Abeysekira, R. Grigg, J. Trocha-Grimshaw, T. J. King, *J. Chem. Soc. Perkin Trans.* **1979**, 2184; c) T. Boschi, S. Licoccia, R. Paolesse, P. Tagliatesta, M. Azarnia, *J. Chem. Soc. Dalton Trans.* **1990**, 463.

[28] For the two previous examples of rhodium(I) complexes with *N*-substituted corroles, see: a) see ref. [27b]; b) A. M. Abegsekira, R.

  0947-6539/01/0705-1054 $ 17.50+.50/0

Grigg, J. Trocha-Grimshaw, V. Viswanatha, *Tetrahedron Lett.* **1976**, 3189.
[29] K. M. Kadish, *Prog. Inorg. Chem.* **1986**, *34*, 435.
[30] J. Bendix, I. J. Dmochowski, H. B. Gray, A. Mahammed, L. Simkhovich, Z. Gross, *Angew. Chem.* **2000**, *112*, 4214; *Angew. Chem. Int. Ed.* **2000**, *39*, 4048.
[31] For the very few cases in which metal carbenes have been unambigiously proven to be the key intermediates, see: a) D. A. Smith, D. N. Reynolds, L. K. Woo, *J. Am. Chem. Soc.* **1993**, *115*, 2511; b) S.-B. Park, N. Sakata, H. Nishiyama, *Chem. Eur. J.* **1996**, *2*, 303; c) H. Nishiyama, N. Soeda, T. Naito, Y. Motoyama, *Tetrahedron: Asymmetry* **1998**, *9*, 2865.
[32] J. K. Wolf, C. G. Hamaker, J.-P. Djukic, T. Kodadek, L. K. Woo, *J. Am. Chem. Soc.* **1995**, *117*, 9194.
[33] For the effect of pyridine on the reduction potential of iron porphyrins, see: L. A. Bottomley, K. M. Kadish, *Inorg. Chem.* **1981**, *20*, 1348.
[34] a) J. Maxwell, T. Kodadek, *Organometallics* **1991**, *10*, 4; b) J. L. Maxwell, K. C. Brown, D. W. Bartley, T. Kodadek, *Science* **1992**, *256*, 1544; c) D. W. Bartley, T. Kodadek, *J. Am. Chem. Soc.* **1993**, *115*, 1656.
[35] B. E. Mann in *NMR of Newly Accesible Nuclei Porphyrins*, *Vol. II* (Ed.: P. Laszlo), Academic Press, New York, **1983**, pp.301–318.
[36] A. W. Johnson, D. Ward, P. Batten, A. L. Hamilton, G. Shelton, *J. Chem. Soc. Perkin Trans.* **1975**, 2070.
[37] N. Haddad, N. Galili, *Tetrahedron: Asymmetry*, **1997**, *8*, 3367.
[38] DENZO: "Processing of X-ray Diffraction Data Collected in Oscillation Mode", Z. Otwinowski, W. Minor, *Methods Enzymol.* **1997**, *276*, 307.
[39] SIR-92: A. Altomare, M. C. Burla, M. Camalli, M. Cascarano, C. Giacovazzo, A. Guagliardi, G. Polidori, *J. Appl. Crystallogr.* **1994**, *27*, 435.
[40] P. T. Beurskens, G. Beurskens, W. P. Bosman, R. de Gelder, S. Garcia-Granda, R. O. Gould, R. Israel and J. M. M. Smits, *DIRDIF-96*, Crystallography Laboratory, University of Nijmegen (The Netherlands), **1996**.
[41] G. M. Sheldrick, *SHELXL-97*, *Program for the Refinement of Crystal Structures from Diffraction Data*, University of Göttingen, Germany, **1997**.

Received: June 7, 2000 [F2530]